Plant Biotechnology Journal Open Access

Plant Biotechnology Journal (2023) **21**, pp. 1560–1576 doi: 10.1111/pbi.14057

The ubiquitin-binding protein MdRAD23D1 mediates drought response by regulating degradation of the proline-rich protein MdPRP6 in apple (*Malus domestica*)

Xiao-Li Zhang†, Xiao-Qing Gong†, Xin-Jian Su, Hai-Xia Yu, Si-Yuan Cheng, Jing-Wen Huang, Dan-Yang Li, Zhao-Long Lei, Ming-jun Li* and Feng-wang Ma*

State Key Laboratory of Crop Stress Biology for Arid Areas/Shaanxi Key Laboratory of Apple, College of Horticulture, Northwest A&F University, Yangling, China

Received 7 October 2022;
revised 13 March 2023;
accepted 1 April 2023.
**Correspondence* (Tel/fax +86-29-87082613; email limingjun@nwsuaf.edu.cn (M.L.) and Tel/fax +86-29-87082648; email fwm64@sina.com, fwm64@nwsuaf.edu.cn (F.M.))
†These authors contribute equally to this study.

Keywords: apple, UBL-UBA protein, drought stress, proline-rich protein, degradation via ubiquitination, free proline accumulation.

Summary

RAD23 (RADIATION SENSITIVE23) proteins are a group of UBL-UBA (ubiquitin-like-ubiquitin-associated) proteins that shuttle ubiquitylated proteins to the 26S proteasome for breakdown. Drought stress is a major environmental constraint that limits plant growth and production, but whether RAD23 proteins are involved in this process is unclear. Here, we demonstrated that a shuttle protein, MdRAD23D1, mediated drought response in apple plants (*Malus domestica*). MdRAD23D1 levels increased under drought stress, and its suppression resulted in decreased stress tolerance in apple plants. Through *in vitro* and *in vivo* assays, we demonstrated that MdRAD23D1 interacted with a proline-rich protein MdPRP6, resulting in the degradation of MdPRP6 by the 26S proteasome. And MdRAD23D1 accelerated the degradation of MdPRP6 under drought stress. Suppression of *MdPRP6* resulted in enhanced drought tolerance in apple plants, mainly because the free proline accumulation is changed. And the free proline is also involved in *MdRAD23D1*-mediated drought response. Taken together, these findings demonstrated that *MdRAD23D1* and *MdPRP6* oppositely regulated drought response. MdRAD23D1 levels increased under drought, accelerating the degradation of MdPRP6. *MdPRP6* negatively regulated drought response, probably by regulating proline accumulation. Thus, "MdRAD23D1-MdPRP6" conferred drought stress tolerance in apple plants.

Introduction

Because plants are unable to move, they encounter diverse environmental stressors, such as drought, high salinity, and extreme temperatures, which inhibit their growth and development (Zhu, 2016). Drought stress is a major environmental constraint on agricultural production, it affects many physiological processes, including photosynthesis, stomatal opening and closing, and the detoxification of reactive oxygen species (ROS). To cope with drought stress, plants have evolved many morphological, physiological, and molecular mechanisms to minimize damage (Farooq *et al.*, 2009; Liu *et al.*, 2019; Ogura *et al.*, 2019; Zhao *et al.*, 2020). For example, ubiquitination, which is a vital way to regulate protein activities and levels at post-translational level in cells, has been shown to mediate drought response in plants. Wheat (*Triticum aestivum*) proteins TaPUB2 and TaPUB3 are E3 ligases that positively regulate *Arabidopsis* response to drought stress (Kim *et al.*, 2022). The UBC27-AIRP3 complex modulates the ABA signalling by promoting ABI1 degradation through ubiquitination in *Arabidopsis* (Pan *et al.*, 2020).

The UBL-UBA (ubiquitin-like-ubiquitin-associated) proteins are ubiquitin receptors and transporters in the ubiquitin-proteasome system (UPS). The UBL domain in UBL-UBA proteins can physically interact with the proteasome receptors Rpn1, Rpn10, and Rpn13 and the UBA domain is linked with ubiquitinated substrates (Finley, 2009; Tsuchiya *et al.*, 2017; Zhang *et al.*, 2009). There are possibly five different types of UBL-UBA proteins, including RAD23 (RADIATION SENSITIVE23; Farmer *et al.*, 2010; Lambertson *et al.*, 1999; Schultz and Quatrano, 1997; Sturm and Lienhard, 1998), DSK2 (DOMINANT SUPPRESSOR OF KAR2; Funakoshi *et al.*, 2002; Kang *et al.*, 2006; Wang *et al.*, 2020), DDI1 (DNA DAMAGE-INDUCIBLE1; Gabriely *et al.*, 2008), NUB1 (NEDD8 ultimate buster 1; Kito *et al.*, 2001), and possibly UBL7 (the Ub-like 7; Liu *et al.*, 2003). After being labelled by the poly-Ub chains, the target protein is recognized and delivered to the 26S proteasome for degradation, and this process is precisely controlled by the UBL-UBA proteins. The vital role of UBL-UBA proteins in protein degradation through the UPS pathway makes them important regulators of growth and stress response in plants. The *Arabidopsis* protein RAD23B regulates pollen development by mediating degradation of KRP1 (KIP-related protein 1; Li *et al.*, 2020a). The rice (*Oryza sativa*) protein OsDSK2a mediates seedling growth and salt response by regulating the degradation of its substrate protein EUI, thus regulating gibberellin metabolism (Wang *et al.*, 2020).

The RAD23 proteins are first known for their role in repairing the damaged DNA caused by UV (Guzder *et al.*, 1998). Plants' RAD23 isoforms can rescue the UV-sensitive phenotype of *rad23D* in yeast, they also contribute to UV tolerance in plants

(Lahari *et al*., 2018; Sturm and Lienhard, 1998). As the UBL-UBA proteins, RAD23 proteins have been proven to be essential in the cell cycle, morphology, and fertility of plants through their delivery of UPS substrates to the 26S proteasome, as evidenced by the severely dwarfed plants or reproductive lethality in different *Arabidopsis* mutants (Farmer *et al*., 2010; Li *et al*., 2020a). Proteomic analysis points to the role of them in apical dominance in *Pinus sylvestris* (Ning *et al*., 2013). Besides, RAD23 proteins appear to be the key factors in pathogen-plant interaction. *Arabidopsis* RAD23C and RAD23D function in insect colonization via interacting with a phytoplasma virulence protein SAP54 (secreted AY-WB protein), which can degrade MADS-box proteins to hijack plant reproduction (MacLean *et al*., 2014). A recent study shows RAD23 proteins interact with bacterium effectors Lso-HPE1 (Lso hypothetical protein effector 1) and CLIBASIA_00460 from *Candidatus Liberibacter solanacearum* and *Candidatus Liberibacter asiaticus*, respectively, thus to promote infection (Oh *et al*., 2022).

Proline-rich proteins (PRPs), a type of cell wall proteins rich in proline and hydroxyproline, play important roles in the drought stress response in plants (Gujjar *et al*., 2018; Liu *et al*., 2018). The proline is an excellent osmolyte, its accumulation helps the cell to maintain the water content and swelling potential, thereby preserving normal cellular function under stresses. It has been clearly demonstrated that plants accumulate proline via the P5CS pathway under stresses (Perez-Arellano *et al*., 2010). And studies show that the accumulation of proline can also be achieved independent of the P5CS pathway, through the degradation of PRP proteins under stress conditions (Barthakur *et al*., 2001; Gujjar *et al*., 2019; Stines *et al*., 1999). The tomato proline-rich protein SlPRP is rapidly down-regulated while the concentration of proline increases in cells under drought stress, helping plants improve the drought resistance (Gujjar *et al*., 2018). Elevated cellular proline content, in turn, may promote PRP levels (Stein *et al*., 2011). Besides the temporary pool of proline, PRPs are also implicated in cell wall signal transduction cascades (Kishor *et al*., 2015). The hybrid PRPs may facilitate signal molecule transport at specific sites in cells (Banday *et al*., 2022). The phosphorylated AZTI (azelaic acid induced 1), a hybrid PRP, may function as a membrane signalling protein in the response to stresses in plants (Pitzschke *et al*., 2014a,b, 2016).

Apple trees are perennial woody fruit trees, and the apple is an economically important fruit around the world. However, drought stress imposes limitations on the development of apple trees and apple production (Mihaljevic *et al*., 2021; Sun *et al*., 2018). The UBL-UBA proteins have been demonstrated to function in various stress responses in different plant species; however, little is known about them in apple plants. In the present study, we identified a UBL-UBA protein MdRAD23D1 from the 'Golden delicious' apple. We demonstrated that *MdRAD23D1* positively regulated the drought response in apple plants by regulating the levels of MdPRP6, which is a PRP (Zhang *et al*., 2021a). MdRAD23D1 can physically interact with MdPRP6, resulting in the degradation of MdPRP6 through the 26S proteasome. In contrast to *MdRAD23D1*, *MdPRP6* negatively regulated the drought response in apple plants. The accumulation of free proline increased in *MdPRP6*-Ri plants and decreased in *MdRAD23D1*-Ri plants under drought, and exogenous proline alleviated drought stress in both *MdPRP6*-cOE calli and *MdRAD23D1*-Ri plants. Thus, we suggested that the MdRAD23D1-MdPRP6 module regulated the drought response of plants, and this process was probably linked to the accumulation of free proline in cells.

Results

The UBL-UBA protein MdRAD23D1 plays a positive role in apples responding to drought stress

We previously identified *MdRAD23* family members in the apple genome (Wang *et al*., 2017), like *Arabidopsis* RAD23 proteins, MdRAD23s also contained the signature UBL domain at the N terminal and UBA domain at the C terminal (Figure S1a). The evolutionary relationship between *Arabidopsis* and apples was analysed, and we found that C and D type RAD23s were close in the phylogenetic tree (Figure S1b). MdRAD23D1, MdRAD23D2, and MdRAD23A were, respectively, collinear with AtRAD23C, AtRAD23D, and AtRAD23A (Figure S1c). Among these three genes, the expression level of *MdRAD23D1* was induced by both ABA treatment and drought stress (Wang *et al*., 2017, Figure 1a). We also examined the MdRAD23D1 protein levels under drought using 'Orin' apple calli. 200 mm mannitol was applied to apple calli to monitor osmotic stress caused by drought, and MdRAD23D1 protein obviously accumulated under mannitol treatment (Figure 1b). To explore the biological function of *MdRAD23D1* in response to drought stress, we obtained three transgenic apple plants with suppressed expression of *MdRAD23D1*, including Ri18, Ri22, and Ri23 (Figure S2a). qPCR analyses showed that the relative expression levels of *MdRAD23D1* decreased by 50%–70% in Ri plants compared with wild type (WT; Figure S2b), without suppression in the expression levels of the other *MdRAD23* members (Figure S2d). The MdRAD23D1 protein levels were also obviously lower in Ri plants when detected using anti-MdRAD23D1 antibody (Figure S2c). After being treated with drought for 8 days, Ri plants exhibited severe leaf wilting, whereas WT was less affected (Figure 1c). Ri leaves drooped away from the stem, to form bigger leaf angles than in WT (Figure 1d). Lower relative water content (RWC) and higher EL were detected in Ri plants than in WT (Figure 1e,f). Furthermore, values for Pn and Fv/Fm were lower in Ri than in WT plants under drought treatment (Figure 1g,h), consistent with weaker fluorescence observed in Ri leaves (Figure 1i). The MDA content was higher in Ri plants (Figure S3a), the stains of 3,3-diaminobenzidine (DAB) and nitro blue tetrazolium (NBT) produced darker colour in Ri than in WT plants (Figure S3b), and higher ROS accumulation was observed in Ri plants by quantitative analyses (Figure S3c,d). Taken together, these results suggest that *MdRAD23D1* plays a positive role in the drought stress response in apple plants.

AtRAD23 proteins have proven to interact with multiple components of the UPS, so we also investigated whether the apple protein MdRAD23D1 has similar interaction. The purified MdRAD23D1-GST protein bound to anti-GST magnetic beads was co-incubated with polyubiquitin chains assembled via K48 or K63 linkages (Ub2-6), and the results showed that MdRAD23D1 bound to both K48- and K63-linked polyubiquitin chains well (Figure 2a). In addition, MdRAD23D1 can interact with MdRPN13, which is a ubiquitin receptor of the 26S proteasome subunit (Husnjak *et al*., 2008), *in vitro* and *in vivo* (Figure 2b–e). Thus, we conclude that MdRAD23D1 associates with the 26S proteasome and is a receptor for ubiquitinated proteins, serving as a shuttle factor in protein degradation via ubiquitination.

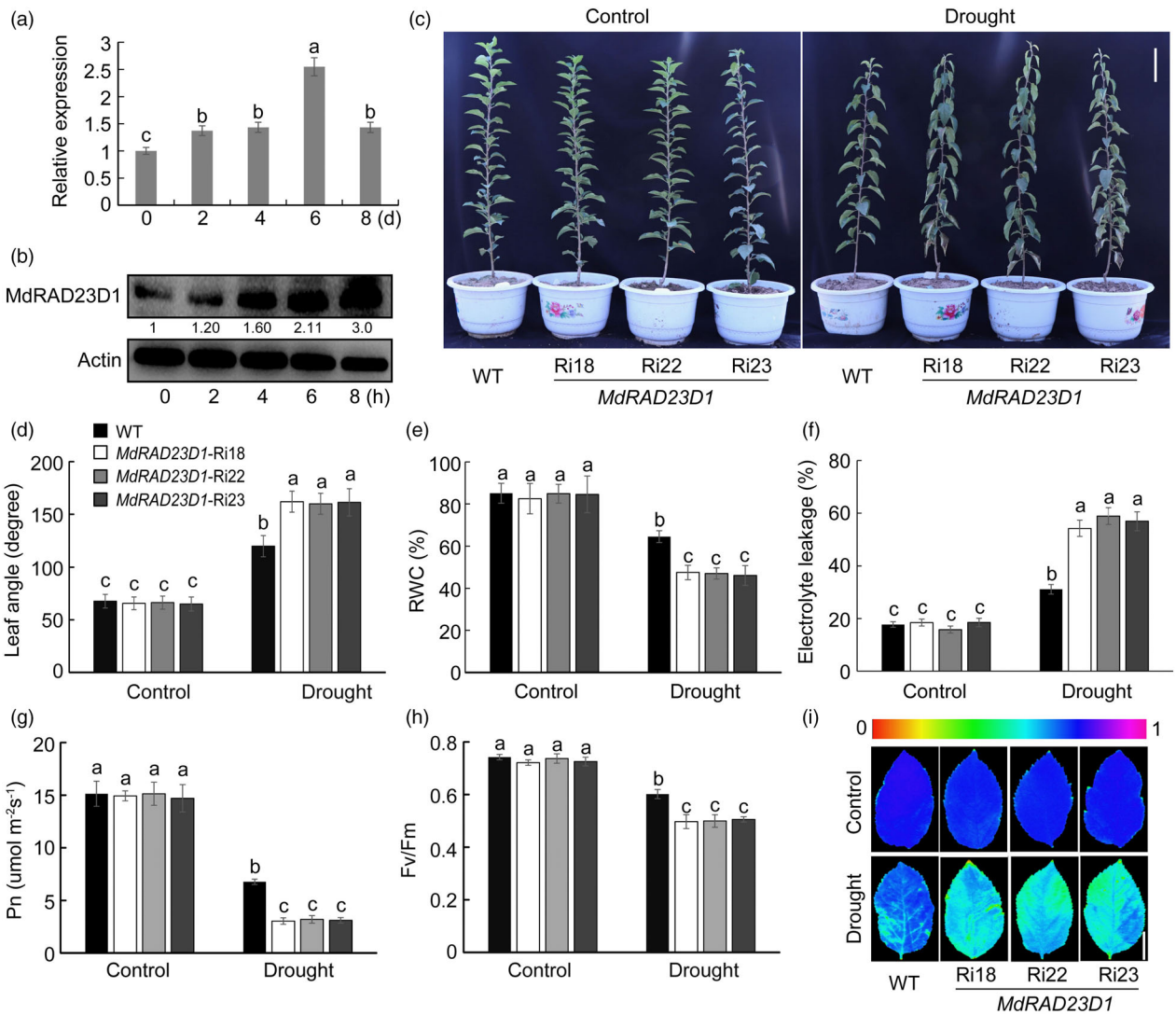

Figure 1 Expression patterns of *MdRAD23D1* and response of *MdRAD23D1* transgenic plants to drought. (a) The expression level of *MdRAD23D1* under drought stress. qPCR was carried out using the GL-3 apple (*Malus domestica*) leaves after drought treatment. (b) MdRAD23D1 levels under drought stress. 200 mM mannitol was applied to the 'Orin' apple (*M. domestica*) calli to monitor drought stress. The calli samples were collected at 0, 2, 4, 6, and 8 h, and a specifically synthesized anti-MdRAD23D1 antibody was used to detect MdRAD23D1 protein levels. MdActin was used as the loading control. The amount of MdRAD23D1 was quantified using an Ultra-sensitive multifunctional imager (Uvitec), and the protein level at 0 h was set to 1. (c) Morphology differences of WT and transgenic apple plants under control and drought conditions. Forty-five-day-old WT and *MdRAD23D1*-Ri plants in the greenhouse were withheld from water for 8 days. The scale bar = 8 cm. (d–i) Leaf angle (d), relative water content (e), electrolyte leakage (f), Net photosynthesis (Pn) (g), Fv/Fm ratio (h), and chlorophyll fluorescence images (i) in WT and transgenic plants with and without drought treatment. The scale bar in (i) = 3 cm. WT, wild type, here we used GL-3 apple (*M. domestic*), which was also used as explants in generating transgenic apple plants; *MdRAD23D1*-Ri18/22/23: transgenic apple plants with suppressed expression of *MdRAD23D1* via RNA-interference. Data are shown as the means ± SD. Different letters indicate significant differences according to the one-way ANOVA followed by Tukey's multiple range test ($P < 0.05$).

MdRAD23D1 interacts with a proline-rich protein, MdPRP6

As mentioned above, *MdRAD23D1* was a positive regulator in drought stress response in apples. As a first approach, we screened an apple cDNA library by the yeast-two hybrid using the CDS of *MdRAD23D1* as the bait. Multiple prey cDNAs identified by the screen expressed a putative 14 KDa PRP, which corresponded to previously named MdPRP6 (Zhang *et al.*, 2021a) and was selected for further study. MdPRP6 has a transmembrane domain and a signal peptide is located in the cell membranes (Zhang *et al.*, 2021a, Figure S4a,b), and MdRAD23D1 is located in the nucleus and the cell membranes (Figure S4a,c), the same location in the cell also suggested the potential relation between MdPRP6 and MdRAD23D1. To further determine the interaction between MdRAD23D1 and MdPRP6, the full-length CDS of *MdPRP6* was cloned using 'Golden Delicious' apple cDNA and fused to the pGADT7 vector. Yeast cells co-transformed with both MdRAD23D1 and MdPRP6 grew well and exhibited blue colour on -Trp/-Leu/-His/-Ade+x-α-gal medium (Figure 3a). When MdRAD23D1 and MdPRP6 were co-expressed in *Nicotiana benthamiana* leaves, the strong luciferase signal was detected

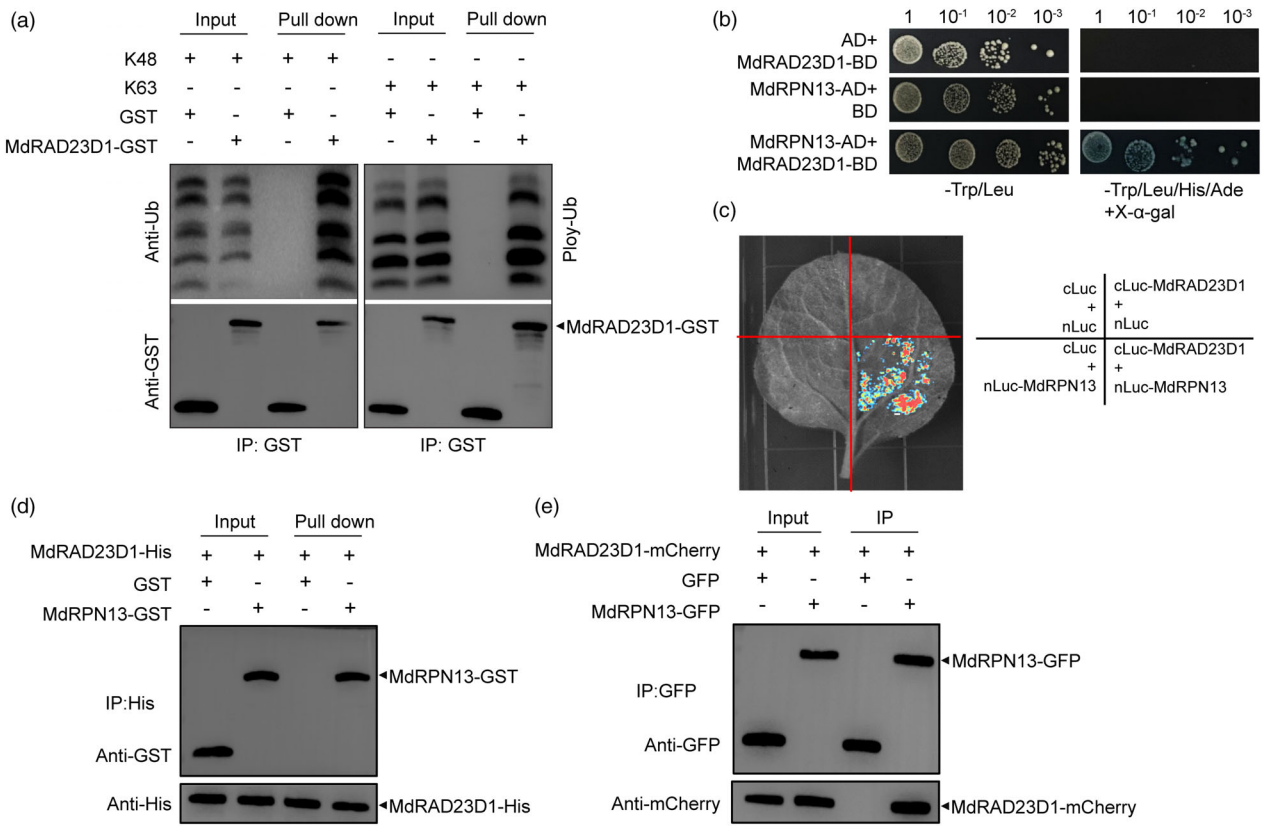

Figure 2 MdRAD23D1 binds poly-ubiquitin (poly-Ub) chains and interacts with the 26S proteasome. (a) Binding of MdRAD23D1 to poly-Ub chains *in vitro*. The *Escherichia coli*–expressed MdRAD23D1-GST fusion protein and GST protein were first incubated with anti-GST magnetic beads and then the mixture was incubated with poly-Ub chains linked via K48 or K63. The bound proteins were eluted and separated by SDS-PAGE and the amount of protein levels were determined by immunoblotting with anti-GST and anti-Ub antibodies. Arrowhead shows the MdRAD23D1-GST protein. (b–e) Interaction analysis of MdRAD23D1 and MdRPN13, a subunit of 26S proteasome via yeast two-hybrid (b), Split-Luc assay (c), Pull-down (d), and Co-IP (e). In yeast two-hybrid assay, the full-length CDS of *MdRAD23D1* and *MdRPN13* was cloned into the pGBKT7 and pGADT7 vectors, respectively. After co-transformation, yeast cells were cultured on SD base/-Leu/-Trp (left) and SD base/-Leu/-Trp/-His/-Ade+x-α-gal (right). In the Split-Luc assay, the full-length CDS of *MdRAD23D1* and *MdRPN13* were cloned into pRI-101-cLuc and pRI-101-nLuc, respectively. The fusion proteins MdRAD23D1-cLuc and MdRPN13-nLuc were transiently co-expressed in *Nicotiana benthamiana* leaves, and the fluorescence signal was observed by an Ultra-sensitive multifunctional imager (Uvitec). In the Pull-down assay, *Escherichia coli*–expressed MdRAD23D1-His protein was first incubated with anti-His magnetic beads and then the mixture was incubated with *E. coli*-expressed MdRPN13-GST or GST. The bound proteins were eluted and detected using anti-GST and anti-His antibodies. In the Co-IP assay, the fusion proteins MdRAD23D1-mCherry and MdRPN13-GFP were transiently co-expressed in *N. benthamiana* leaves, and the total proteins were extracted and immunoprecipitated with anti-GFP magnetic beads. Immunoblotting was performed with anti-GFP and anti-mCherry antibodies.

with an Ultra-sensitive multifunctional imager (Figure 3b). In the pull-down assay, we incubated purified MdRAD23D1-GST with MdPRP6-His, and the interaction between them was detected after pull-down (Figure 3c). We also performed Co-IP assay using *N. benthamiana* leaves co-expressing MdRAD23D1-GFP and MdPRP6-Flag, and the immunoblot analyses showed that MdRAD23D1 interacted with MdPRP6 (Figure 3d). Together, these results demonstrate that MdRAD23D1 interacts with MdPRP6 *in vitro* and *in vivo*.

MdPRP6 negatively regulates the drought response of apple

Previously we demonstrated that *MdPRP6* was expressed in leaves, stems, and roots of apple plants, and it played a role in plants responding to heat, salt, and low nitrogen stresses (Zhang *et al*., 2021a, 2022, 2023). Here, we further examined the spatial expression patterns of *MdPRP6* by *in situ* hybridization in different tissues. Strong signals of *MdPRP6* were detected in vascular tissues, such as xylem and phloem, implying that *MdRPR6* might affect the water uptake of apple plants (Figure 4a). In contrast to *MdRAD23D1*, the expression levels of *MdPRP6* were inhibited by drought stress (Figure 4b). We examined the MdPRP6 protein levels under drought using *MdPRP6-Flag* transgenic apple calli (*MdPRP6*-cOE in Figure S5a–c). MdPRP6 protein levels strongly decreased after 8 h of 200 mM mannitol treatment (Figure 4c), without a corresponding decrease in *MdPRP6* expression levels (Figure S5d).

To gain a better understanding of the role of *MdPRP6* under drought stress, we generated another transgenic line with suppressed expression of *MdPRP6* in GL-3 via RNA interference silencing (Ri3 in Figure S6a,b), without a decrease in expression levels of the other *MdPRP* members (Figure S6c, Ri1 and Ri2 were previously obtained in Zhang *et al*., 2022). After 8 days of plant exposure to drought stress, leaves of WT were substantially more wilting than those of Ri plants (Figure 5a,b). Values for leaf angles and EL were lower in Ri plants than in WT plants (Figure 5c,e),

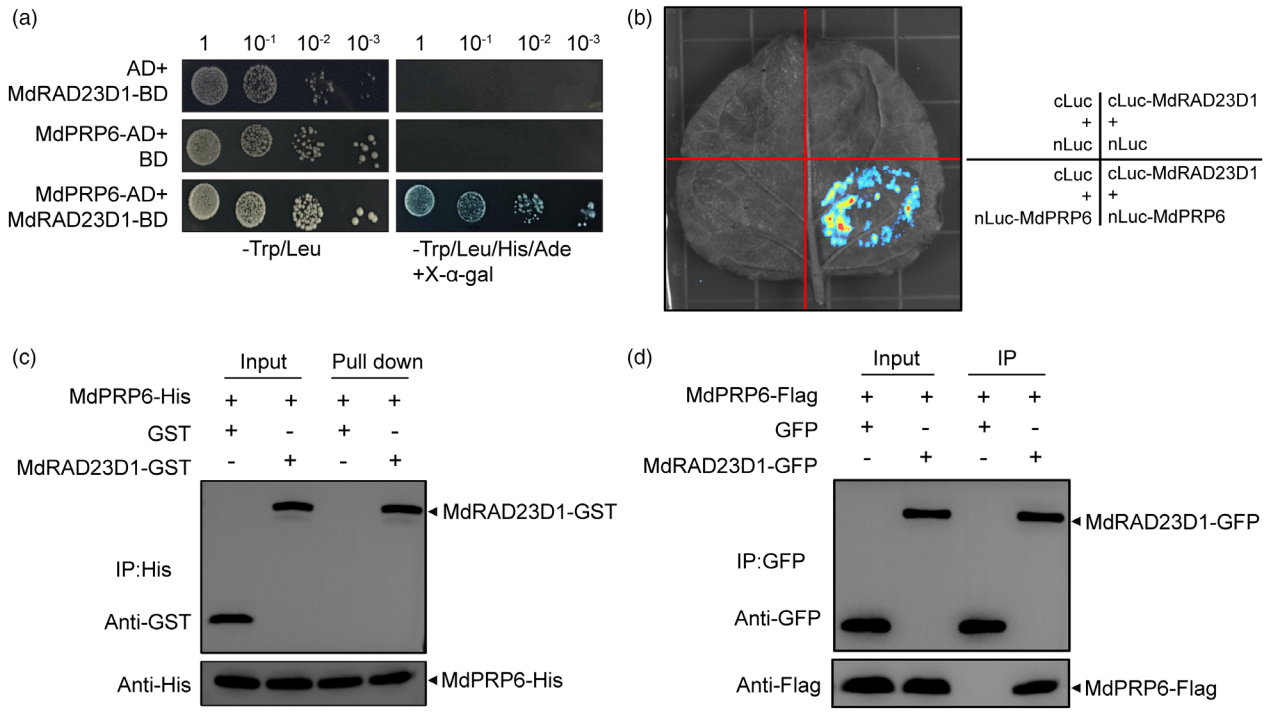

Figure 3 MdRAD23D1 interacts with MdPRP6 *in vivo* and *in vitro*. (a) Yeast two-hybrid assays. The full-length CDS of *MdRAD23D1* and *MdPRP6* were cloned into pGBKT7 and pGADT7 vectors, respectively. Co-transformed yeast cells were grown on SD-Trp/-Leu and SD-Trp/-Leu/-His/-Ade+X-α-gal medium. (b) The Split-Luc assay. The full-length CDS of *MdRAD23D1* and *MdPRP6* were cloned into pRI-101-cLuc and pRI-101-nLuc, respectively. The fusion proteins MdRAD23D1-cLuc and MdPRP6-nLuc were transiently co-expressed in *Nicotiana benthamiana* leaves, and the fluorescence signal was observed by an Ultra-sensitive multifunctional imager (Uvitec). (c) Pull-down assays. *Escherichia coli*–expressed MdPRP6-His protein was first incubated with anti-His magnetic beads and then the mixture was incubated with *E. coli*-expressed GST or MdRAD23D1-GST. The bound proteins were eluted and detected using anti-GST and anti-His antibodies. (d) Co-IP assay. The fusion proteins MdRAD23D1-GFP and MdPRP6-Flag were transiently co-expressed in *N. benthamiana* leaves, and the total proteins were extracted and immunoprecipitated with anti-GFP magnetic beads. Immunoblotting was performed with anti-GFP and anti-Flag antibodies.

whereas values for RWC were higher in Ri plants (Figure 5d). Under drought treatment, Ri plants had higher Pn and Fv/Fm values than WT plants, as well as stronger chlorophyll fluorescence (Figure 5f–h). We also noticed that the MDA content was higher in WT plants than in Ri plants (Figure S7a). The leaves of WT plants were stained more densely with DAB and NBT compared with Ri leaves (Figure S7b). Ri plants under drought stress also had consistently lower H_2O_2 and O_2^- contents (Figure S7c,d). These results demonstrate that *MdPRP6* negatively regulates the drought stress response in apple plants.

MdRAD23D1 affects the protein levels of MdPRP6

We analysed the protein levels of MdRAD23D1 in *MdPRP6*-cOE and *MdPRP6*-cRi (Figure S5e,f) calli, using the anti-MdRAD23D1 antibody. We found that the altered expression of *MdPRP6* did not affect MdRAD23D1 levels (Figure S8a). To analyse whether MdRAD23D1 affects MdPRP6 levels, we generated *MdRAD23D1*-cOE (Figure S9a–c) and *MdRAD23D1*-cRi (Figure S9d–f) transgenic apple calli, and then expressed *MdPRP6-Flag* in *MdRAD23D1*-cOE and *MdRAD23D1*-cRi calli (*MdRAD23D1*-cOE/*MdPRP6*-cOE and in *MdRAD23D1*-cRi/*MdPRP6*-cOE Figure S10a–d). We found that when MdRAD23D1 levels increased, MdPRP6-Flag levels decreased, and *vice versa* (Figure S8b), indicating that MdRAD23D1 might function upstream of MdPRP6.

Given the shuttle function of MdRAD23D1, it probably transports ubiquitylated MdPRP6 to the 26S proteasome. As a first approach, we detected the MdPRP6 levels in *MdPRP6-Flag* transgenic calli supplied with or without MG132. Without MG132, MdPRP6-Flag levels decreased over time. In contrast, when MG132 was added, MdPRP6-Flag was more stable (Figure 6a). When we incubated MdPRP6-His with protein extracts from WT or *MdRAD23D1*-Ri plants, MdPRP6-His protein levels decreased more slowly in *MdRAD23D1*-Ri plants than in WT, and MG132 inhibited the decrease in MdPRP6-His levels in both two (Figure 6b). We also employed different co-transgenic calli in the assay. At each time point, MdPRP6-Flag was most abundant in *MdRAD23D1*-cRi/*MdPRP6*-cOE calli and least abundant in *MdRAD23D1*-cOE/*MdPRP6*-cOE calli (Figure 6c). We used anti-Flag and anti-Ubi antibodies to detect the ubiquitination levels of MdPRP6 in the co-transgenic calli and found that changes in MdRAD23D1 levels did not affect the ubiquitination levels of MdPRP6-Flag (Figure 6d). In summary, these data demonstrate that MdPRP6 would be degraded by the UPS, and MdRAD23D1 promotes its degradation.

MdRAD23D1 promotes MdPRP6 degradation under drought stress

MdRAD23D1 promoted the degradation of MdPRP6, and drought stress also inhibited the expression of *MdPRP6*. To further investigate the role of their association in regulating apple drought response, a cell-free degradation assay and *in vivo* protein degradation assay were carried out to measure MdPRP6

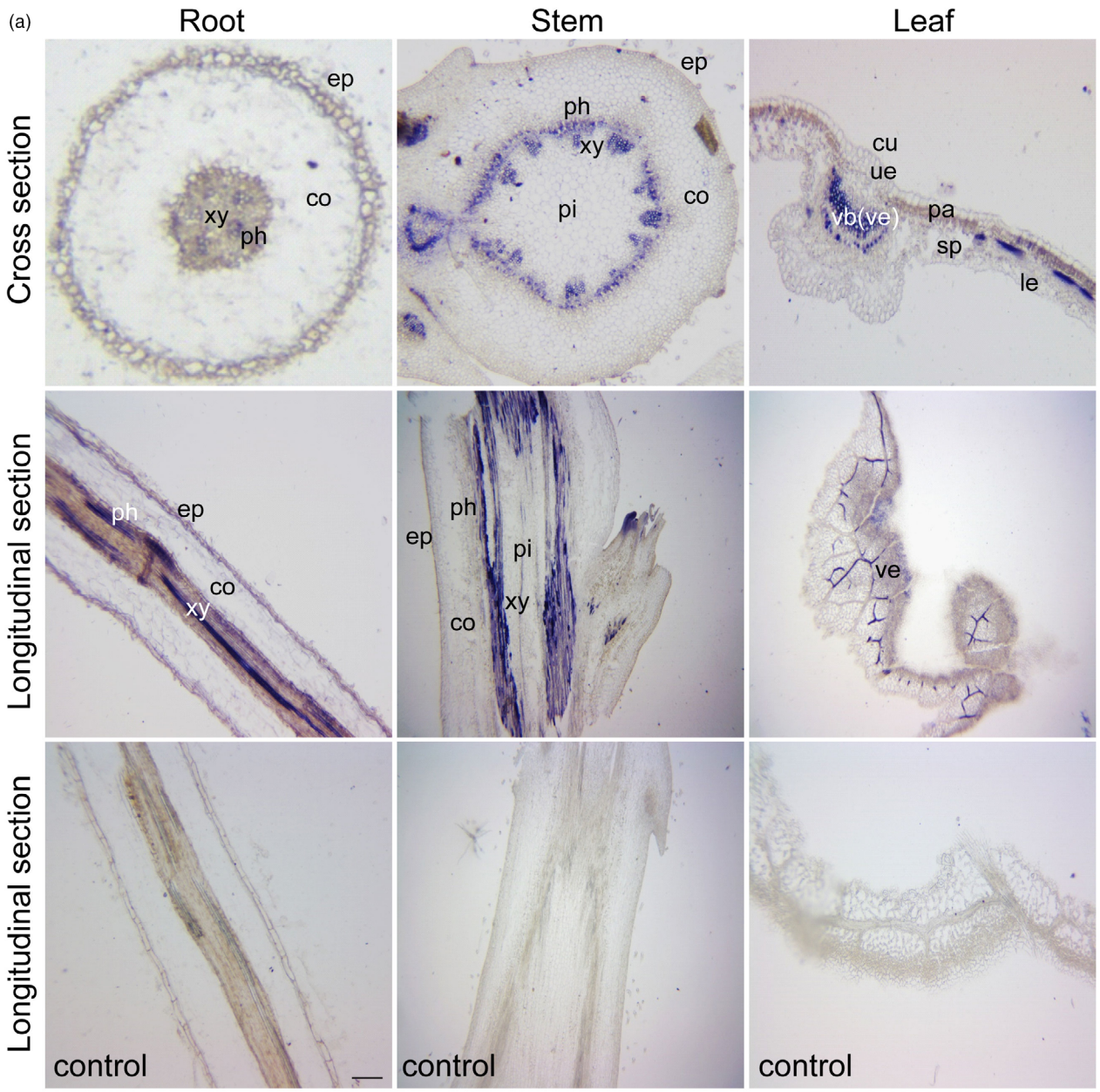

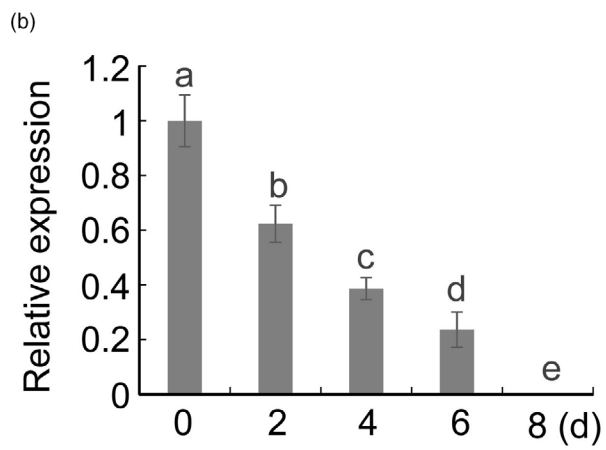

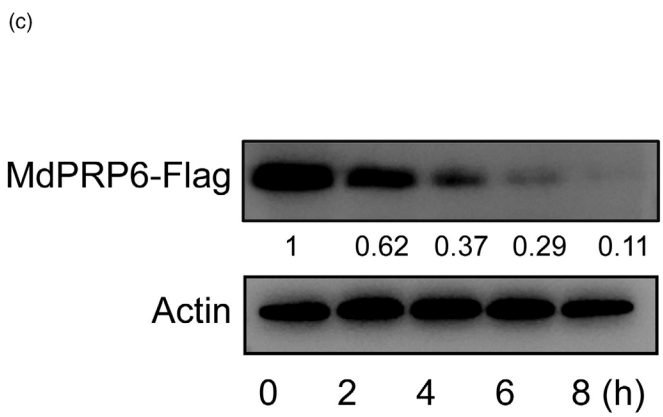

Figure 4 Expression patterns of *MdPRP6*. (a) *In situ* hybridization of *MdPRP6* in roots, stems, and leaves of GL-3 apple (*Malus domestica*). ep, epidermis; xy, xylem; ph, phloem; pi, pith; co, cortex; cu, cuticle; ue, upper epidermis; le, lower epidermis; pa, palisade mesophyll cells; sp, spongy mesophyll cells; vb, vascular bundle; ve, vein. The scale bar = 100 μm. (b) The expression level of *MdPRP6* under drought stress. qPCR was carried out using the GL-3 apple leaves after drought treatment. (c) MdPRP6 levels under drought stress. 200 mM mannitol was applied to the transgenic apple calli ('Orin' calli, *M. domestica*) expressed 35S::*MdPRP6-Flag* to monitor drought stress. The *MdPRP6-Flag* calli were cultured on MS medium containing 200 mM mannitol and 75 μM CHX. The calli sample was collected at 0, 2, 4, 6 and 8 h and immunoblotting was performed with anti-Flag antibody. MdActin was used as the loading control. The amount of MdPRP6 was quantified using an Ultra-sensitive multifunctional imager (Uvitec), and the protein level at 0 h was set to 1. Data in (b) are shown as the means ± SD. Different letters indicate significant differences according to a one-way ANOVA followed by Tukey's multiple range test ($P < 0.05$).

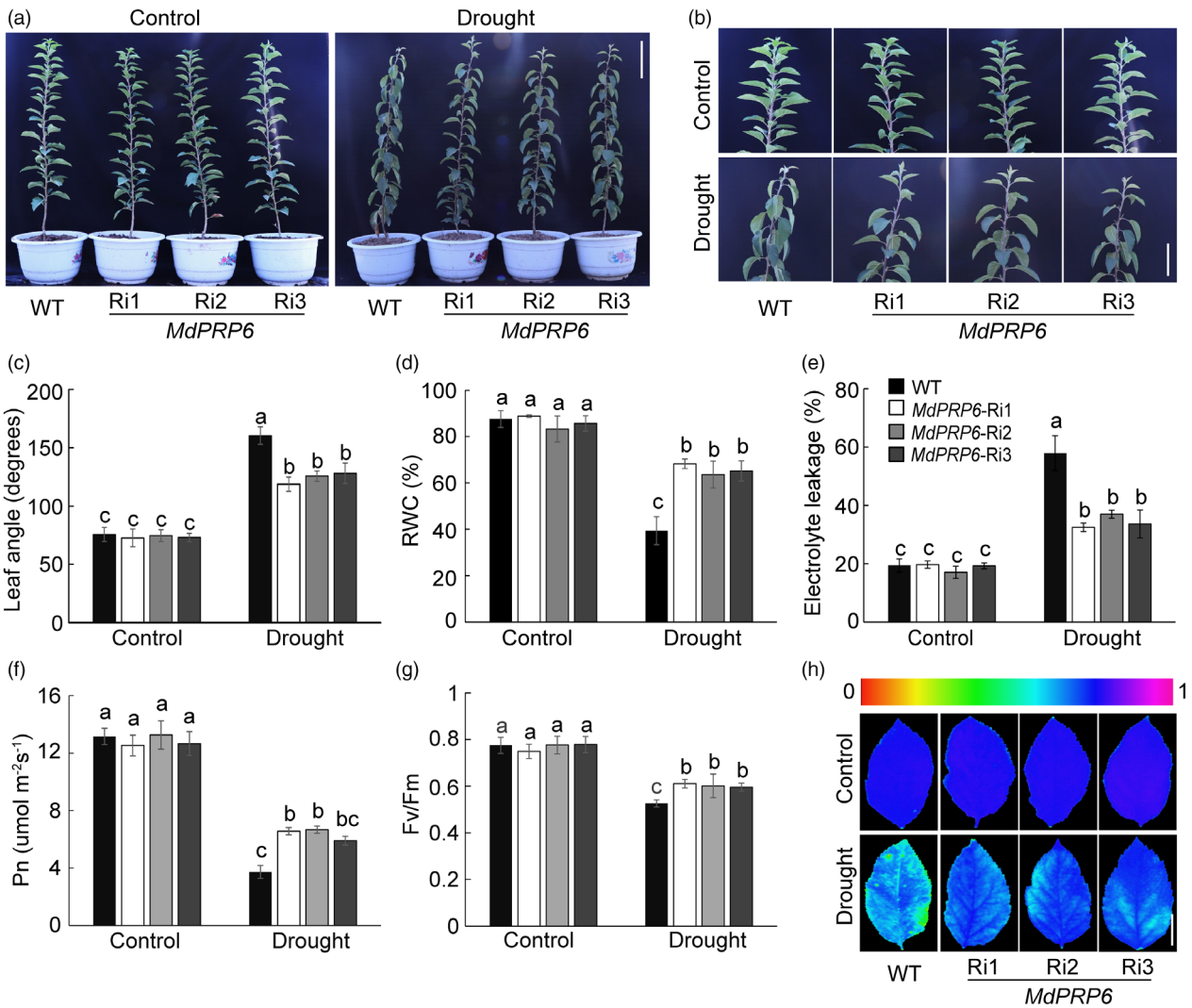

Figure 5 *MdPRP6* negatively regulates the drought tolerance of apple plants. (a, b) Morphology differences in whole plants (a) and top enlarged view (b) of WT and transgenic apple plants under control and drought conditions. Forty-five-day-old WT and *MdPRP6*-Ri plants in the greenhouse were withheld from water for 8 days. The Scale bars in (a) and (b) were 15 cm and 7 cm, respectively. (c–h) Leaf angle (c), relative water content (d), electrolyte leakage (e), net photosynthesis (Pn) (f), Fv/Fm ratio (g), and chlorophyll fluorescence images (h) in WT and *MdPRP6*-Ri plants with and without drought treatment. The Scale bar in (h) = 3 cm. Data are shown as the means ± SD. Different letters indicate significant differences according to the one-way ANOVA followed by Tukey's multiple range test ($P < 0.05$). WT, wild type, here we used GL-3 apple (*Malus domestic*), which was also used as explants in generating transgenic apple plants; *MdPRP6*-Ri1/2/3, transgenic apple plants with suppressed expression of *MdPRP6* via RNA-interference.

levels. When MdPRP6-His fusion protein was incubated with protein extracts from WT or *MdRAD23D1*-Ri plants under drought stress, MdPRP6-His protein levels significantly decreased after 3 h of drought stress treatment in WT plants but after 5 h of drought stress treatment in *MdRAD23D1*-Ri plants (Figure 7a). We also detected the levels of MdPRP6-Flag in co-transgenic

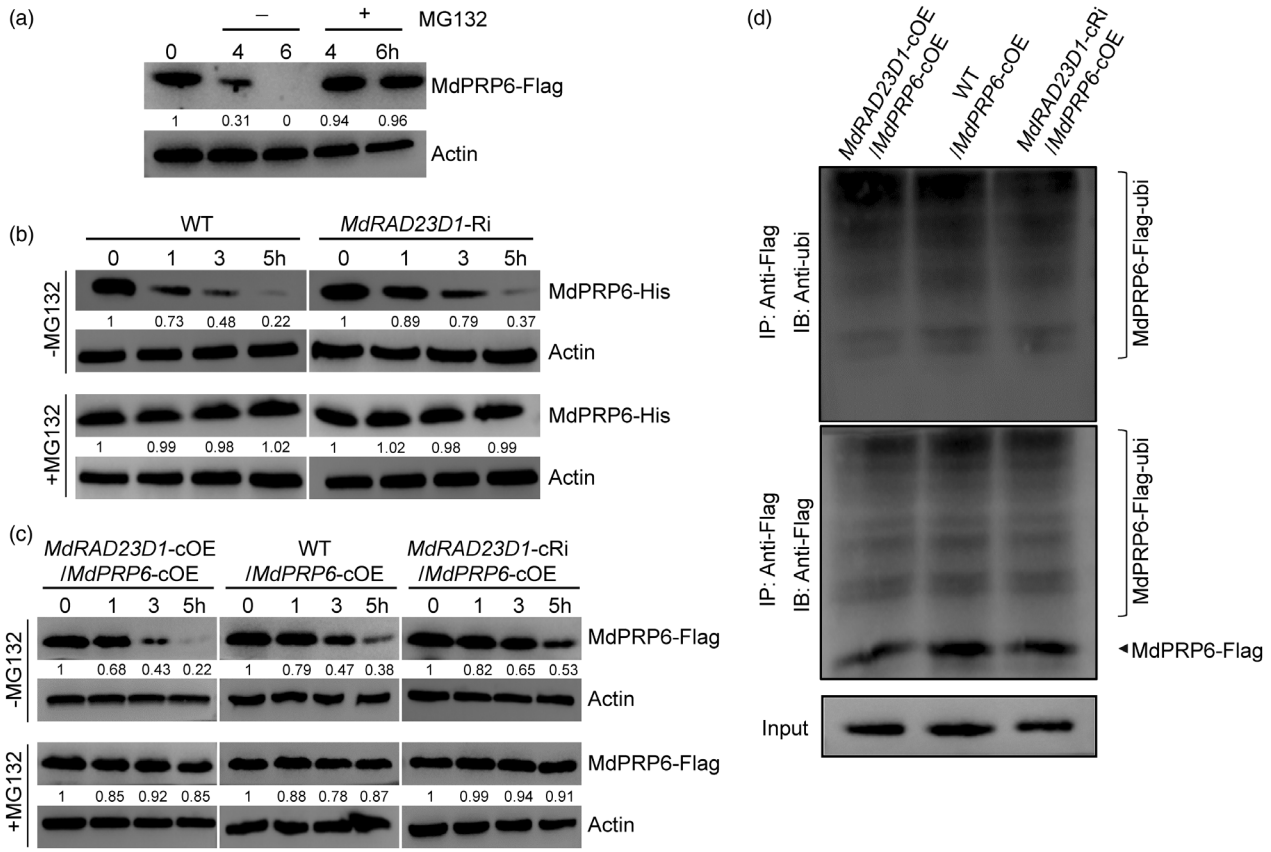

Figure 6 MdRAD23D1 promotes the degradation of MdPRP6. (a) Effects of MG132 on MdPRP6 degradation. The transgenic apple calli expressed 35S::*MdPRP6-Flag* were treated with 75 μM CHX with (+) or without (−) 50 μM MG132 for the indicated time, and the amount of MdPRP6-Flag was determined using anti-Flag antibody. (b) Cell-free degradation assays in apple plants. The *Escherichia coli*–expressed MdPRP6-His protein was incubated with the protein extracts from WT or *MdRAD23D1*-Ri apple plants with or without MG132, and then immunoblotting was performed using anti-His antibody at the indicated time points. (c) MdRAD23D1 affects the degradation of MdPRP6 *in vivo*. Total proteins separately were extracted from the WT/*MdPRP6*-cOE, *MdRAD23D1*-cOE/*MdPRP6*-cOE, and *MdRAD23D1*-cRi/*MdPRP6*-cOE transgenic apple calli after treated with 75 μM CHX with or without MG132. The immunoblotting was performed with anti-Flag antibody. (d) Ubiquitination of MdPRP6 *in vivo*. The total proteins were separately extracted from the same three calli in (c) and immunoprecipitated using anti-Flag magnetic beads. The MdPRP6-Flag protein was detected with anti-ubi antibody and anti-Flag antibody. WT in (b), wild type, here we used GL-3 apple (*Malus domestica*), which was also used as explants in generating transgenic apple plants; *MdRAD23D1*-Ri, transgenic apple plants with suppressed expression of *MdRAD23D1* via RNA interference; *MdRAD23D1*-cOE/*MdPRP6*-cOE, transgenic apple calli co-expressed 35S::*MdRAD23D1-HA* and 35S::*MdPRP6-Flag*; *MdRAD23D1*-cRi/*MdPRP6*-cOE, transgenic apple calli with suppressed expression of *MdRAD23D1* via RNA-interference, and co-expressed with 35S::*MdPRP6-Flag*; WT/*MdPRP6*-cOE, transgenic apple calli expressed 35S::*MdPRP6-Flag*. All the transgenic apple calli was generated using 'Orin' calli (*M. domestica*). MdActin was used as the loading control (a–c) or input control (d). The amounts of proteins were quantified using an Ultra-sensitive multifunctional imager (Uvitec), and the protein levels at 0 h were set to 1.

apple calli treated with 200 mM mannitol. MdPRP6-Flag band was difficult to detect at 3 h in the *MdRAD23D1*-cOE/*MdPRP6*-cOE calli, and at 5 h in the WT/*MdPRP6*-cOE calli, but it was still detectable at 5 h in the *MdRAD23D1*-cRi/ *MdPRP6*-cOE calli (Figure 7b).

We examined the drought sensitivity of different transgenic calli. The size of *MdRAD23D1*-cOE calli was larger than the size of WT calli and *MdRAD23D1*-cRi calli under 200 mM mannitol treatment (Figure S11a,b). We then expressed *MdPRP6-Flag* in the above three transgenic calli and treated the co-trangenic calli with 200 mM mannitol (Figure 7c). When *MdPRP6* was over-expressed alone (WT/*MdPRP6*-cOE), the fresh weight of transgenic calli decreased upon treatment with 200 mM mannitol. However, the fresh weight of transgenic calli was higher when *MdRAD23D1* was also overexpressed (*MdRAD23D1*-cOE/*MdPRP6*-cOE), and it was lowest when the expression of *MdRAD23D1* was suppressed (*MdRAD23D1*-cRi/*MdPRP6*-cOE; Figure 7d). These results suggest that *MdRAD23D1* affects the drought tolerance of *MdPRP6*.

The free proline contributes to the drought stress response in *MdPRP6* transgenic apple plants

Previously, we found that *MdPRP6* affects the free proline accumulation under salt stress (Zhang *et al.*, 2023), and the same physiological changes were also detected under drought stress. The *MdPRP6*-Ri plants contained higher levels of free proline than WT plants under drought (Figure 8a). To verify whether the proline is implicated in *MdPRP6*-mediated drought response, we tested the stress response of *MdPRP6* transgenic calli after being treated with proline. The results showed that when *MdPRP6* was overexpressed, the free proline content decreased in transgenic calli under 200 mM mannitol treatment,

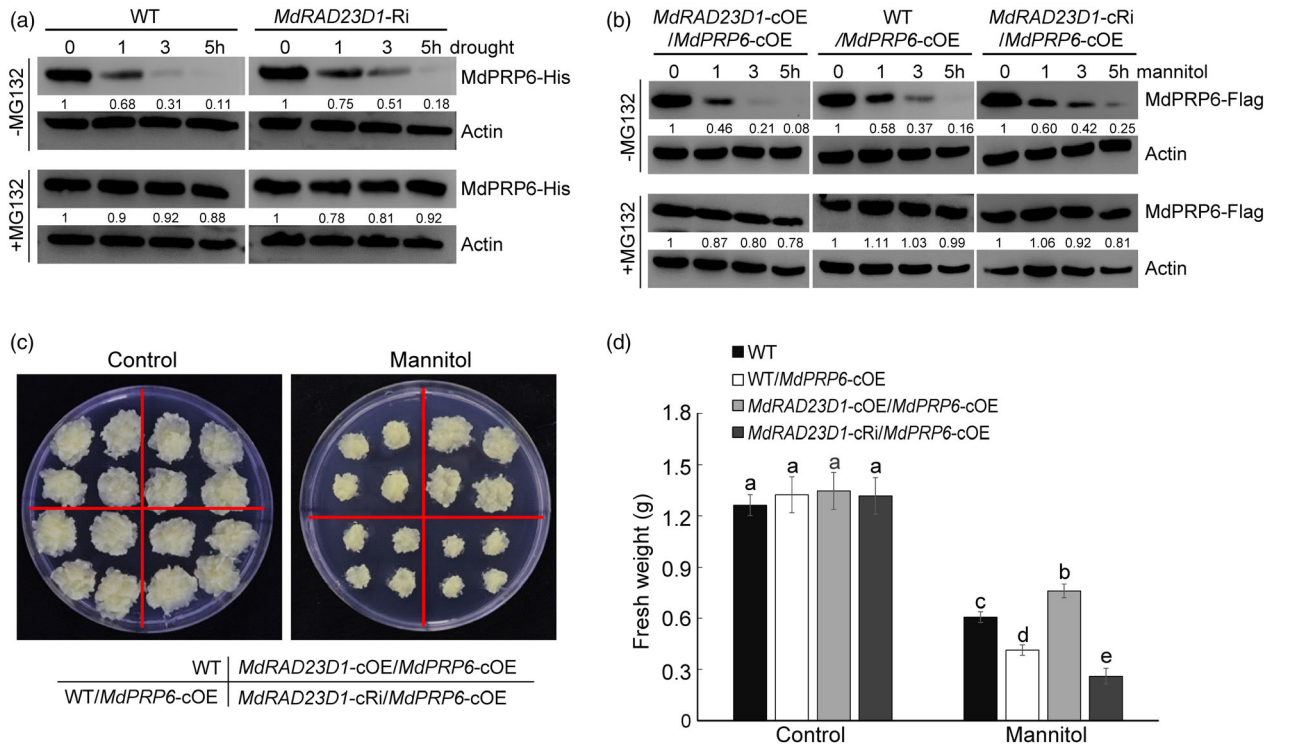

Figure 7 MdRAD23D1-promoted MdPRP6 degradation affects drought tolerance. (a) Promotion of MdPRP6 degradation by MdRAD23D1 under drought *in vitro*. The *Escherichia coli*–expressed MdPRP6-His protein was incubated with the total proteins extracted from WT or *MdRAD23D1*-Ri apple plants with or without MG132 under drought treatment. The amount of MdPRP6-His was determined with anti-His antibody. (b) Promotion of MdPRP6 degradation by MdRAD23D1 under drought *in vivo*. 200 mM mannitol was applied to apple calli to monitor osmatic stress caused by drought. Total proteins were extracted from WT/*MdPRP6*-cOE, *MdRAD23D1*-cOE/*MdPRP6*-cOE, and *MdRAD23D1*-cRi/*MdPRP6*-cOE transgenic apple calli treated with 75 μM CHX with or without MG132. The immunoblotting was performed with anti-Flag antibody. (c) Morphology differences of apple calli grown on MS medium with or without 200 mM mannitol for 20 days. (d) The fresh weights of apple calli. WT in (a), wild type, here we used GL-3 apple (*Malus domestica*), which was also used as explants in generating transgenic apple plants; WT in (b–d), wild type, here we used 'Orin' apple calli (*Malus domestica*), which was also used as explants in generating transgenic apple calli; *MdRAD23D1*-Ri, transgenic apple plants with suppressed expression of *MdRAD23D1* via RNA-interference; *MdRAD23D1*-cOE/*MdPRP6*-cOE, transgenic apple calli co-expressed 35S::*MdRAD23D1-HA* and 35S::*MdPRP6-Flag*; *MdRAD23D1*-cRi/*MdPRP6*-cOE, transgenic apple calli with suppressed expression of *MdRAD23D1* via RNA-interference, and co-expressed with 35S::*MdPRP6-Flag*; WT/*MdPRP6*-cOE, transgenic apple calli expressed 35S::*MdPRP6-Flag*. MdActin was used as the loading control in (a) and (b). The amounts of proteins were quantified using an Ultra-sensitive multifunctional imager (Uvitec), and the protein levels at 0 h were set to 1. Data in (d) are shown as the means ± SD. Different letters indicate significant differences according to a one-way ANOVA followed by Tukey's multiple range test ($P < 0.05$).

and *vice versa* (Figure 8b). After treated with exogenous proline, the proline content was almost the same in *MdPRP6*-cOE calli and WT under 200 mM mannitol treatment (Figure 8c), and no difference in calli size and fresh weight were observed between *MdPRP6*-cOE calli and WT (Figure 8d,e). These results indicate that the proline in *MdPRP6* transgenic plants is implicated with *MdPRP6*-mediated drought response.

Given the promoted MdPRP6 degradation by MdRAD23D1 under drought stress, we reasoned that the proline content would also change in *MdRAD23D1* transgenic materials. So we measured it and found that the proline content was less in *MdRAD23D1*-Ri plants than in WT under drought (Figure 8f). When we applied exogenous proline to *MdRAD23D1*-Ri plants under drought treatment, the proline content was similar between *MdRAD23D1*-Ri plants and WT (Figure 8g). And the proline-treated *MdRAD23D1*-Ri plants were as tolerant as the proline-treated WT plants, no difference was observed in the performance, EL, and MDA content between them under drought treatment (Figure 8h–j). We also examined the proline content in *MdRAD23D1* transgenic calli and tested their stress response treated with proline. The results showed that when *MdRAD23D1* was overexpressed, the proline content increased in transgenic calli under 200 mM mannitol treatment, and *vice versa* (Figure S12a). After treated with exogenous proline, the proline content was almost the same in *MdRAD23D1*-cRi calli and WT under 200 mM mannitol treatment (Figure S12b), and no difference in calli size and fresh weight were observed between *MdRAD23D1*-cRi calli and WT (Figure S12c,d). In addition, we measured the free proline content in co-transgenic calli. When *MdRAD23D1* was overexpressed (*MdRAD23D1*-cOE/*MdPRP6*-cOE), the free proline content significantly increased under mannitol treatment, much higher than in WT and WT/*MdPRP6*-cOE calli. When it was inhibited (*MdRAD23D1*-cRi/*MdPRP6*-cOE), the free proline content decreased, lower than in WT/*MdPRP6*-cOE calli (Figure S12e). All these results demonstrate that the free proline is also involved in *MdRAD23D1*-mediated drought response.

Discussion

Drought is an emerging global problem that limits plant growth and crop yield (Iglesias *et al.*, 2011). The apple is an economically

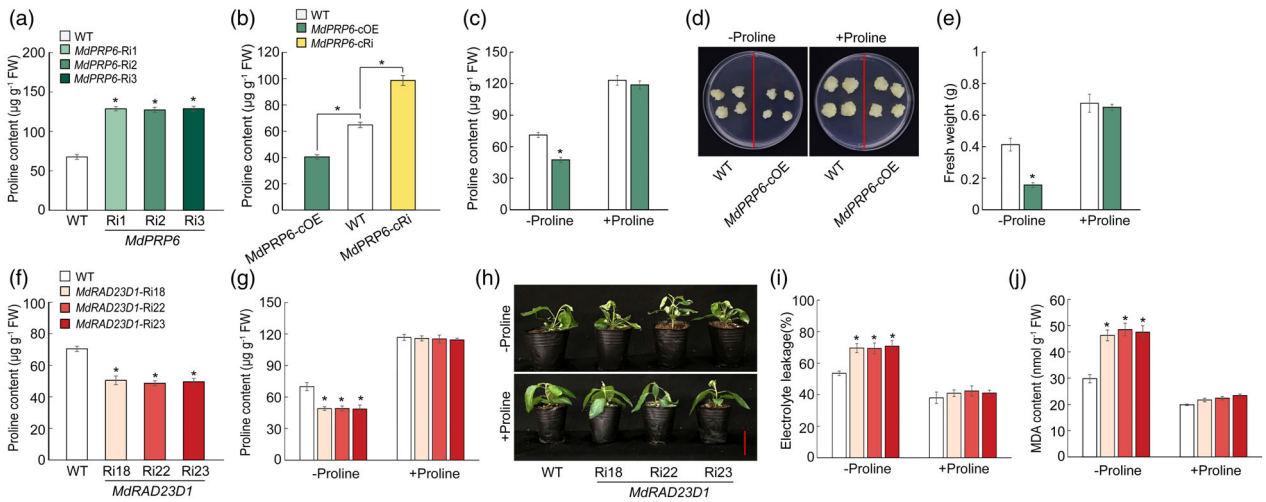

Figure 8 Effects of proline metabolism on the drought response of WT, *MdPRP6*, and *MdRAD23D1* transgenic apple plants. (a) The free proline content in WT and *MdPRP6*-Ri apple plants under drought stress. (b) The free proline content in WT and *MdPRP6* transgenic apple calli. (c–e) The free proline content (c), phenotypes analyses (d), and fresh weight (e) in WT and *MdPRP6*-cRi calli supplied with or without proline under 200 mM mannitol treatment. (f) The free proline content in WT and *MdRAD23D1*-Ri apple plants under drought stress. (g–j) The free proline content (g), phenotypes analyses (h), electrolyte leakage (i), and MDA content (j) in WT and *MdRAD23D1*-Ri plants supplied with or without proline under drought stress. The scale bar = 5 cm in (h). WT in (a) and (f–j), wild type, here we used GL-3 apple (*Malus domestic*), which was also used as explants in generating transgenic apple plants; *MdPRP6*-Ri1/2/3, transgenic apple plants with suppressed expression of *MdPRP6* via RNA interference; *MdRAD23D1*-Ri18/22/23: transgenic apple plants with suppressed expression of *MdRAD23D1* via RNA-interference. WT in (b–e), wild type, here we used 'Orin' apple calli (*Malus domestica*), which was also used as explants in generating transgenic apple calli; *MdPRP6*-cOE, transgenic apple calli expressed 35S::*MdPRP6-Flag*; *MdPRP6*-cRi, transgenic apple calli with suppressed expression of *MdPRP6* via RNA-interference. Data are shown as the means ± SD. Asterisks indicate significant differences between WT and transgenic materials exposed to the same treatment (*, $P < 0.05$).

important fruit worldwide, and drought stress seriously reduces the yield and quality of apples in China and around the world. Plants have evolved multiple physiological mechanisms to cope with drought stress. For example, increasing root branching and density to promote water uptake (Henry *et al*., 2011), decreasing stomatal density in leaves to reduce water loss (Hughes *et al*., 2017), enhancing autophagic activity to improve water use efficiency (Jia *et al*., 2021b). They also changed at the molecular level in response to drought. For example, the E3 ligase MdMIEL1 degrades MdBBX7, thus conferring drought tolerance in apples (Chen *et al*., 2022). Apple SERRATE directly interacts with MdMYB88 and MdMYB124 to regulate their expression, it also regulates the microRNA biogenesis, thus regulating drought response (Li *et al*., 2020b). In this study, we uncovered a new regulatory module, MdRAD23D1-MdPRP6, in the response to drought stress in apple plants. Our results suggest that MdRAD23D1 could interact with MdPRP6 and promote its degradation via the UPS under drought stress, which modulates stress response in apple plants.

RAD23s are UBL-UBA proteins, and they are involved in plant growth and development as well as the responses to various stresses in different species. *Arabidopsis* RAD23B regulates pollen development by mediating degradation of KRP1 (Li *et al*., 2020a). Dsk2 interacts with Irc22 and confers salt stress tolerance in yeast (Ishii *et al*., 2014). Recombinant Rad23 protein can protect HeLa cells from UV irradiation and inhibits apoptosis after exposure to UV irradiation (Li *et al*., 2013). Our previous research revealed that the six *MdRAD23s* were induced by various stresses in apples (Wang *et al*., 2017). Here, we found that the expression of *MdRAD23D1* was strongly induced by drought and osmotic stress (Figure 1), implying that *MdRAD23D1* may play a role in the response to drought in apples. Using different transgenic materials, we observed that *MdRAD23D1* positively regulated drought stress response of apple plants. The *MdRAD23D1*-Ri plants were much more sensitive to drought, as evidenced by their wilted leaves, higher EL values, MDA content, and ROS accumulation, as well as their lower RWC and Photosynthesis efficiency compared with WT plants (Figure 1, Figure S3). In addition, the *MdRAD23D1*-cRi calli were less tolerant to osmotic stress, but *MdRAD23D1*-cOE calli were more tolerant, as revealed by the changed size and fresh weight under mannitol treatments (Figure S11).

Expression of *MdRAD23D1* improved the drought resistance of apple plants. In addition to the physiological changes, we also examined this phenomenon at the molecular level. We performed a yeast two-hybrid screening assay to identify proteins that interacted with MdRAD23D1 and identified a proline-rich protein MdPRP6, which was further confirmed by *in vivo* and *in vitro* experiments (Figure 3). RAD proteins are the ubiquitin shuttles of the UPS, and they are connected to the 26S proteasome by their UBL domains and to the ubiquitinated protein by the UBA domains (Farmer *et al*., 2010; Ishii *et al*., 2006; Liang *et al*., 2014). MdRAD23D1 was the apple protein homologous to RAD proteins and also functioned as a transporter (Figure 2). Proteins that interact with the shuttles might be ubiquitinated and can be degraded via UPS (Hara *et al*., 2005; Zhang *et al*., 2021b, c). We found that when MdRAD23D1 levels increased, MdPRP6 levels decreased (Figure S8). MdPRP6 was degraded via UPS and MdRAD23D1 promoted its degradation without affecting its ubiquitination levels (Figure 6a–d). In addition, MdRAD23D1-promoted MdPRP6 degradation affected the stress response of apple calli treated

with mannitol (Figure 7). Together, we hypothesized that this was a possible molecular mechanism for how MdRAD23D1 promoted drought response in apple plants.

When we considered the degradation of MdPRP6 as a potential reason to explain the regulation of *MdRAD23D1* under drought stress, we met with a new problem: what was the role of *MdPRP6* in apple plants experiencing drought stress? It is known that PRPs are a type of cell wall structural protein that play important roles in coping with various stresses in different species (Li *et al.*, 2016; Mellacheruvu *et al.*, 2016; Priyanka *et al.*, 2010; Seo *et al.*, 2011). *HyPRP1* negatively regulates salt and oxidative stress responses in tomatoes (*Solanum lycopersicum*) by modulating sulfite metabolism (Li *et al.*, 2016). The expression of *GhHyPRP4* was down-regulated in response to drought, salt, and ABA treatment (Huang *et al.*, 2011). In this study, we found that *MdPRP6* also played a negative role in the response to drought stress in apple plants. Its expression was inhibited by drought stress (Figure 4b,c), and when we suppressed the expression of *MdPRP6* in apple plants, we found that *MdPRP6*-Ri plants were much more tolerant to drought stress than WT plants (Figure 5, Figure S7).

The proline-rich secreted protein FOCL1 involves in the stomata development in the drought response in *Arabidopsis* (Hunt *et al.*, 2017). The SlPRP in tomatoes is down-regulated by drought stress and may regulate the free proline content in the cellular response to drought stress (Gujjar *et al.*, 2018). *MdPRP6* negatively regulated drought response, so how it works? Proline is an important osmolyte in plants responding to drought stress (Huang *et al.*, 2021; Wang *et al.*, 2021). We found that the cellular free proline is implicated with *MdPRP6*-mediated drought response (Figure 8a–e). As previously observed under salt stress (Zhang *et al.*, 2023), we found that the P5CS activity was also higher in *MdPRP6*-Ri plants under drought (Figure S13a,b), suggesting that *MdPRP6* might affect the P5CS pathway in accumulating proline under stresses. Besides the P5CS pathway, the proline can also be produced from degradation of the PRPs to counteract stress (Barthakur *et al.*, 2001; Gujjar *et al.*, 2018, 2019; Raymond and Smirnoff, 2002; Saikia *et al.*, 2020). We also tested this possibility by silencing *MdP5CS* via VIGS in *MdPRP6*-Ri plants (Figure S14), and then we found it failed to totally destroy the proline accumulation and drought resistance in *MdPRP6*-Ri plants (Figure S13c–f). So, the increased proline contents in *MdPRP6*-Ri plants might be derived from both the P5CS pathway and MdPRP6 degradation.

Drought stress quickly induces the synthesis of ABA, the increased ABA then activates its signal transduction, thus activating cellular response (Furihata *et al.*, 2006; Ma *et al.*, 2009; Park *et al.*, 2009; Umezawa *et al.*, 2009). *MdRAD23D1* is induced by ABA treatment (Wang *et al.*, 2017), and *MdPRP6* is also induced by ABA in 24 h (Zhang *et al.*, 2021a), but it was inhibited since day two (Figure S15a). So what would happen if blocking the ABA signalling? We treated *MdPRP6*-Ri plants with NDGA (Nordihydroguaiaretic acid), one of the ABA biosynthesis inhibitors, to block the synthesis of ABA, thus blocking its signalling (Cutler *et al.*, 2010; Lin *et al.*, 2021; Figure S15b,c). The results showed that NDGA eliminated response differences between WT and *MdPRP6*-Ri plants (Figure S15d–g). It seems that *MdPRP6* also worked in an ABA-dependent manner under drought, just like many other drought-responsive genes (Collin *et al.*, 2020; Joo *et al.*, 2019). However, although decreased ABA level would inhibit its signal, NDGA is not a specific inhibitor to block its signal, so *MdPRP6* might also function upstream of the ABA biosynthesis. How does ABA or ABA signalling interact with MdPRP6? More work is needed to clarify these findings.

In conclusion, we demonstrated that *MdRAD23D1* and *MdPRP6* function oppositely in the response of apple plants to drought. MdRAD23D1 positively regulates drought response and promotes the degradation of MdPRP6 via UPS under drought stress. *MdPRP6* negatively regulates drought response. It can affect the accumulation of cellular free proline, possibly via both the P5CS pathway and its degradation under drought. The increased free proline contents then contribute to the improved drought resistance of apple plants. In addition, the ABA pathway might also function in *MdPRP6*-mediated drought response (Figure 9). Our findings suggest that "MdRAD23D1-MdPRP6" is a new type of regulon in the response to drought in apple plants.

Experimental procedures

Analysis of phylogenetic relationships

RAD23 proteins were identified from the apple (GDR; https://www.rosaceae.org/) and *Arabidopsis* genomes (Tair; https://www.arabidopsis.org/). All amino acid sequences were analysed to identify domains using Pfam (http://pfam.xfam.org/) and SMART (http://smart.embl-heidelberg.de/) with the default parameters. DNAMAN software was used to compare the amino acid sequences of RAD23 from *Arabidopsis* and apples. A phylogenetic tree of RAD23s was then constructed by MEGA 6.06 software according to the neighbour-joining approach, and the test parameter bootstrap was repeated 1000 times. We then constructed a homologous relationship map between the *RAD23* genes of apple and *Arabidopsis* using Dual Synteny Plotter software (Chen *et al.*, 2020).

Plant materials and growth conditions

Tissue-cultured GL-3 apple (*Malus domestica*) plants and 'Orin' apple (*M. domestica*) calli were used in this study. GL-3 and transgenic apple plants were cultured as described by Sun *et al.* (2018) and Zhou *et al.* (2019). Briefly, after rooting, tissue-cultured plants were transferred to the plastic pots (10 × 10 × 10 cm) filled with a mixture of organic substrate/vermiculite/perlite (3 : 1 : 1, v : v : v) and placed in a light incubator (23 °C, 16/8 h light/dark). Thirty days later, they were transferred to larger plastic pots (30 × 18 cm) with the same weight mixture of soil/sand/organic matter (v : v : v, 5 : 1 : 1) and placed in a greenhouse.

'Orin' apple calli were cultured on MS medium with 1.5 mg L^{-1} 2,4-D (2,4-Dichlorophenoxyacetic acid) and 0.4 mg L^{-1} 6-BA (N-(Phenylmethyl)-9H-purin-6-amine) in continuous darkness.

Vector construction and genetic transformation

To construct overexpression (OE) vectors, the full-length CDS of *MdRAD23D1* was separately inserted into three vectors: pRI-101 (with a GFP tag), pRI-101 (with a mCherry tag), and pGWB415 (with a HA tag). The full-length CDS of *MdPRP6* was separately cloned into pCambia2300 (with a Flag tag) and pCambia2300 (with a GFP tag). The full-length CDS of *MdRPN13* was cloned into the vector pCambia2300 (with a GFP tag). To generate RNA interference (Ri) vectors, a 295 bp sequence from the 5′ end of *MdRAD23D1* (218–512 bp) was cloned into the pHellsgate2 vector, a 200 bp sequence at the 5′ end of *MdPRP6* (1–200 bp) was cloned into the pK7GWIWG2D vector. All constructed OE and Ri vectors were introduced into *Agrobacterium tumefaciens* strain EHA105 by the freeze and thaw method.

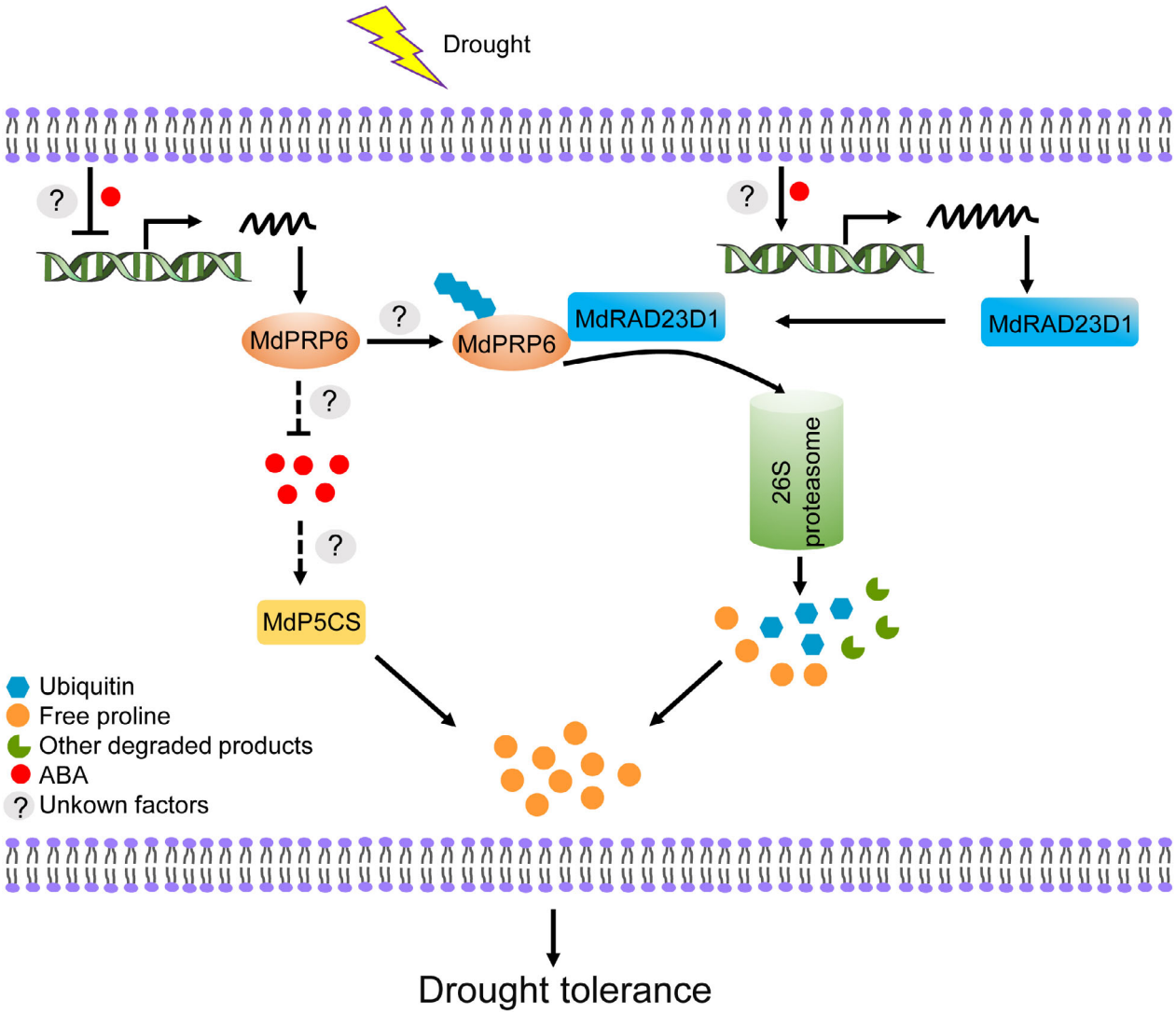

Figure 9 A proposed mechanism model of 'MdRAD23D1-MdPRP6' regulon in apples under drought. Under drought stress, MdRAD23D1 protein levels increase, accelerating MdPRP6 degradation via 26S proteasome, there by the MdPRP6 protein levels decrease under drought. The free proline from MdPRP6 degradation might contribute to build up a high cellular free proline content. In addition, MdPRP6 affects the P5CS activity, might via the ABA pathway, to regulate proline synthesis. The increased free proline then makes apple plants resist drought stress.

Genetic transformation of apple plants (using GL-3 as explants) and calli (using 'Orin' as explants) were carried out as described by Dai *et al*. (2013) and Li *et al*. (2012). The transgenic lines were screened on a medium containing 50 mg/L kanamycin or 15 mg/L hygromycin B (only for apple calli). The resistant materials were verified by PCR. Expression levels of *MdRAD23D1* and *MdPRP6* in the positive transgenic materials were analysed by qPCR, and MdRAD23D1 levels were detected using a specifically synthesized antibody, MdPRP6 levels were detected using an anti-Flag antibody. All the primers are listed in Table S1.

RNA extraction and gene expression analysis

The expression levels of *MdRAD23D1* and *MdPRP6* under drought stress were determined using the leaves of GL-3, and the protein levels of MdRAD23D1 and MdPRP6 under drought stress were detected using WT ('Orin') calli and *MdPRP6*-cOE calli (expressed 35S::*MdPRP6-Flag*), respectively. For qPCR, total RNA was extracted from apple leaves or calli as described by Huo *et al*. (2020). The synthesis of the first-strand cDNA was performed using RevertAid First Strand cDNA Synthesis Kit (Thermo Scientific, Waltham, MA). qPCR was conducted on a LightCycler 96 system (Roche, Basel, Switzerland). *MDH* (encoding malate dehydrogenase) was used as an internal reference to calculate the relative expression levels for each gene. Three biological replicates and three technical replicates were performed for each experiment. All the primers used for qPCR are listed in Table S1. For separately analysing the protein levels of MdRAD23D1 and MdPRP6 under drought stress, the total protein was extracted from different calli samples treated with 200 mM mannitol at 0, 2, 4, 6, and 8 h, and then immunoblot analyses were performed using anti-MdRAD23D1 antibody and anti-Flag antibody, respectively.

In situ hybridization assay

In situ hybridizations of *MdPRP6* in apple plants were conducted as previously described by Geng *et al*. (2018) with slight

modification. Briefly, the roots, stems, and leaves of GL-3 were collected and immediately fixed in formalin-aceto-alcohol (FAA) solution (4% formaldehyde, 10% acetic acid, and 50% ethanol). The tissues were decolorized, embedded in Paraffin, and sliced. The glass slides were then placed at 37 °C for 8-12 h. Xylene was used to remove all the wax, and gradient ethanol and DEPC water were used to dehydrate the samples. Finally, the glass slides were digested in 1 μg/mL protease K at 37 °C. The glass slides were incubated with the probe at 42 °C overnight and then rinsed with washing buffer at 23 and 65 °C before being stored in TE buffer. The probes are listed in Table S1.

Drought stress treatments

The transgenic and WT (here we used GL-3) apple plants were cultured as described above. After growth in the greenhouse for 45 days, all apple plants were fully irrigated and the drought treatment was performed as previously described (Jia *et al*., 2021a). The apple plants of uniform size were selected and randomly divided into two groups as follows: (1) the control group, which was watered every 2 days; (2) the drought group, which received no water for 8 days. Samples were then collected at 0, 2, 4, 6, and 8 d and stored at −80 °C for subsequent experiments. There were three independent biological replicates for each group, containing at least 60 plants in total.

The transgenic and WT (here we used 'Orin') apple calli were cultured as described above. To monitor drought stress, 200 mM mannitol was added to the medium, and 2-week-old WT and transgenic apple calli of equal weight (0.1 g) were used in the treatments. Samples were then collected at 20 days and stored at −80 °C for subsequent experiments. There were four independent replicates for each experiment.

VIGS (virus-induced gene silencing)-mediated silencing of *MdP5CS* in apple plants was performed according to previous methods (Sasaki *et al*., 2011; Zhu *et al*., 2022) with minor modification (the detailed method is included in Figure S14). After confirmation, all the positive plants were treated with drought stress for 15 days by stopping watering.

For the proline or NDGA treatments, 1-month-old *MdRAD23D1*-Ri apple plants or *MdPRP6*-Ri apple plants were, respectively, applied with 5 mM proline or 10 μM NDGA and treated with drought stress for 15 days. Exogenous proline or NDGA was sprayed on leaves every 2 days. In addition, the transgenic and WT apple calli (0.1 g) were grown on MS medium treated with 200 mM mannitol with or without 5 mM proline for 20 days. The samples were harvested at the end of treatment and stored at −80 °C for subsequent experiments. There were four independent replicates for each experiment.

Measurement of physiological traits and photosynthetic parameters

Electrolyte leakage (EL) was measured according to Sun *et al*. (2018). The total chlorophyll was extracted with 80% acetone, and a UV-2250 spectrophotometer (Shimadzu, Kyoto, Japan) was used to measure the chlorophyll content according to Liu *et al*. (2021). RWC was calculated following the method of Jia *et al*. (2021b). The leaf angle was the angle between the straight part of the leaf and the stem. A CIRAS-3 portable photosynthesis system (CIRAS-3; PP Systems, Amesbury, MA) was used to measure photosynthetic parameters. The chlorophyll fluorescence was detected using a chlorophyll fluorescence imaging system (IMAGING-PAM, WALZ, Bavaria, Germany).

NBT and DAB were used to detect the accumulation of superoxide radical (O_2^-) and hydrogen peroxide (H_2O_2), respectively (Fryer *et al*., 2002). Free proline content, as well as MDA, H_2O_2, O_2^- and P5CS activity were detected using their corresponding detection kits (Suzhou Comin Biotechnology Co., Ltd., Suzhou, China).

Screening of the cDNA library via the yeast two-hybrid (Y2H) assay

To identify proteins that interact with MdRAD23D1, the CDS of *MdRAD23D1* was cloned into the pGBKT7 to construct a MdRAD23D1-BD vector. The cDNA library was constructed using mixed samples of apple roots, stems, and leaves, according to the protocol of Clontech. Then MdRAD23D1-BD was expressed in the Y2H Gold (Clontech) strain to test self-activation. Screening of the cDNA library and yeast transformation were performed according to the protocol. When analysing the interaction between MdRAD23D1 and MdRPN13, MdRAD23D1 and MdPRP6, the CDS of *MdPRP6* and *MdRPN13* were cloned into the pGADT7 to generate the MdPRP6-AD and MdRPN13-AD constructs. And then MdRAD23D1-BD and MdPRP6-AD or MdRPN13-AD were co-transformed into yeast strain Y2H Gold according to the protocol. All positive clones were selected on SD base/-Leu/-Trp/-His/-Ade + x-α gal (5-Bromo-4-chloro-3-indoxyl-α-D galactopyranoside) to confirm the interactions.

Subcellular localization of MdRAD23D1 and MdPRP6

MdRAD23D1 was transiently expressed in tobacco (*N. benthamiana*) leaves and *Arabidopsis* protoplasts to analyse its localization in cells, MdPRP6 was transiently expressed in onion epidermal cells and *Arabidopsis* protoplasts to analyse its localization in cells. The detailed method is included in Figure S4.

Pull-down assays

The CDS of *MdRAD23D1*, *MdPRP6*, and *MdRPN13* were cloned into the pET28a (with a His tag) and pGEX4T-1(with a GST tag) vectors to generate the recombined constructs pET28a-35S::*MdRAD23D1-His*, pGEX-4 T-1-35S::*MdRAD23D1-GST*, pET28a-35S::*MdPRP6-His*, and pGEX-4T-1-35S::*MdRPN13-GST*. To study protein expression, 100 ng of each plasmid was separately transformed into *Escherichia coli* BL21 (DE3) and fusion proteins were induced by 1 mM isopropyl β-D-1- thiogalactopyranoside (IPTG) for 12 h at 16 °C. Then, the fusion proteins bound to His magnetic beads were incubated with MdRPN13-GST (or MdRAD23D1-GST) fusion proteins in binding buffer A containing 50 mM Tris–HCl, pH 8.0, 200 mM NaCl, 1 mM EDTA, 1 mM DTT (DL-Dithiothreitol), 10 mM $MgCl_2$, 1% Nonidet P-40, 1 mM PMSF (phenylmethylsulfonyl fluoride), and 1× complete protease inhibitor cocktail (P9599; Sigma-Aldrich, St. Louis, MO, USA) for at least 2 h at 23 °C with gentle shaking. Finally, the proteins were eluted according to the protocol of Beyotime and immunoblotted using anti-GST and anti-His antibodies (Yeasen, Shanghai, China).

Split-luciferase assays

The CDS of *MdRAD23D1* was cloned into pRI-101-cLuc, and the CDS of *MdPRP6* and *MdRPN13* were cloned pRI-101-nLuc to generate cLuc-*MdRAD23D1*, nLuc-*MdPRP6*, and nLuc-*MdRPN13*. These constructs were transformed into EHA105 and then injected into the leaves of *N. benthamiana*. The luciferase expression signals were detected with an Ultra-sensitive multi-functional imager (Uvitec, Cambridge, UK).

Co-Immunoprecipitation (Co-IP) assays

To perform the Co-IP assays, different combinations of proteins were co-expressed in *N. benthamiana* leaves via injection, including pRI-101-35S::*GFP* and pCambia2300-35S::*MdPRP6-Flag*, pRI-101-35S::*MdRAD23D1-GFP* and pCambia2300-35S::*MdPRP6-Flag*, pCambia2300-35S::*GFP* and pRI-101-35S::*MdRAD23D1-mCherry*, and pRI-101-35S::*MdRAD23D1-mCherry* and pCambia2300-35S::*MdRPN13-GFP*. Total proteins were extracted using an extraction buffer containing 50 mM Tris–HCL, 150 mM NaCl, 5 mM EDTA, 1% NP-40, 10% glycerol, 1 mM PMSF, 5 mM DTT, and 1× complete protease inhibitor cocktail. Anti-GFP magnetic beads were used for Co-IP assays according to the manufacturer's manuals (Beyotime, Shanghai, China). Briefly, 10 μL pre-prepared anti-GFP magnetic beads were added to each 500 μL of protein sample and incubated at 4 °C overnight with gentle shaking. The beads were then washed three times with extraction buffer, and the immunoprecipitated proteins were eluted according to the protocol of Beyotime. Protein blot analysis was performed using anti-GFP, anti-Flag, or anti-mCherry antibodies (Yeasen, Shanghai, China).

Ubiquitin chain binding assays

The purified MdRAD23D1-GST protein was first incubated with anti-GST magnetic beads at 4 °C overnight according to the manufacturer's manuals (Beyotime, Shanghai, China). Then, the mixture was incubated with 20 μL purified Lys-48 (K48) or Lys-63 (K63) linked chains (Ub2-6) (Ubbiotech, Changchun, China) in buffer A at 23 °C for 2 h. Then, the bound proteins were washed three times in buffer A and eluted according to the protocol of Beyotime. Finally, the eluted proteins were immunoblotted using anti-GST antibody (Yeasen) and anti-Ub antibody (CST, Denver, MA, USA).

Protein degradation and *in vivo* ubiquitination assay

For the cell-free assay, DMSO or 50 μM MG132 (stock solution prepared with 0.5% DMSO) was added to apple plants 1 h before extraction. The total protein of WT or *MdRAD23D1*-Ri transgenic apple plant was extracted using degradation buffer containing 25 mM Tris–HCl (pH 7.5), 10 mM NaCl, 10 mM $MgCl_2$, 4 mM PMSF, 5 mM DTT, and 10 mM ATP (Yang *et al.*, 2021). The protein extracts were incubated with *E. coli* expressed MdPRP6-His at 23 °C for specific time points and detected by immunoblotting with an anti-His antibody (Yeasen).

For the *in vivo* degradation assay, DMSO or 50 μM MG132 (stock solution prepared with 0.5% DMSO) and 75 μM CHX (Cycloheximide, a protein synthesis inhibitor) were added to *MdPRP6* transgenic and co-transgenic apple calli. The samples were harvested at specific time points and total protein was extracted as described above. The extracted protein was immunoblotted using anti-Flag antibody.

For the *in vivo* ubiquitination assay, the co-transgenic apple calli were treated with 50 μM MG132 for 10 h before extraction. Then, the extracted total proteins were immunoprecipitated with anti-Flag magnetic beads (Beyotime) and immunoblotted with anti-Flag antibody (Yeasen) and anti-Ub antibody (CST).

All the proteins were quantified using an Ultra-sensitive multifunctional imager (Uvitec), and the protein levels at 0 h were set to 1. MdActin protein was used as the loading control or input control.

Statistical analysis

All data were analysed using IBM SPSS Statistics software (version 20; SPSS Inc., Chicago, IL). One-way ANOVA and Tukey's multiple-range tests or Student's *t*-test were used to evaluate significant differences ($P < 0.05$).

Accession numbers

The *Arabidopsis* sequences were found from the *Arabidopsis* Information Resource (TAIR) site and the accession numbers were as follows: AtRAD23A (AT1G16190), AtRAD23B (AT1G79650), AtRAD23C (AT3G02540), and AtRAD23D (AT5G38470). The apple sequences data used in this study can be downloaded from Genome Database for Rosaceae (GDR) site and the accession numbers were as follows: MdRAD23A (MD09G1229800), MdRAD23B (MD17G1228500), MdRAD23C1 (MD13G1043000), MdRAD23C2 (MD16G1043900), MdRAD23D1 (MD17G1076200), MdRAD23D2 (MD09G1087400), MdPRP1 (MD07G1116600), MdPRP2 (MD02G1209700), MdPRP3 (MD02G1023200), MdPRP4 (MD04G1086500), MdPRP5 (MD04G1087300), MdPRP6 (MD15G1126700), MdPRP7 (MD06G1062200), MdPRP8 (MD06G1062000), MdPRP9 (MD15G1166100), and MdRPN13 (MD16G1238000).

Acknowledgements

This work was supported by the National Key Research and Development Program of China (2018YFD1000300), the National Natural Science Foundation of China (31972391), the Fundamental Research Funds for the Central Universities (2452022118), the earmarked fund for the China Agricultural Research System (CARS-27) and the Key S&T Special Projects of Shannxi Province (2020zdzx03-01-02). And the authors are grateful to Dr Zhihong Zhang from Shenyang Agricultural University for providing tissue-cultured GL-3 apple plants, as well as the Horticulture Science Research Center at the College of Horticulture, NWAFU for their technical support in this work.

Conflict of interest

No conflicts of interest were declared.

Author contributions

X-QG, X-LZ, and F-WM conceived and designed the experiments. X-LZ, X-JS, and H-XY performed the research. S-YC, J-WH, D-YL and Z-LL analysed the data, and X-LZ, X-QG, and F-WM wrote the paper. X-QG, F-WM, and M-JL revised the paper.

Data availability

Research data are not shared.

References

Banday, Z.Z., Cecchini, N.M., Speed, D.J., Scott, A.T., Parent, C., Hu, C.T., Filzen, R.C. *et al.* (2022) Friend or foe: hybrid proline-rich proteins determine how plants respond to beneficial and pathogenic microbes. *Plant Physiol.* **190**, 860–881.

Barthakur, S., Babu, V. and Bansal, K.C. (2001) Over-expression of osmotin induces proline accumulation and confers tolerance to osmotic stress in transgenic tobacco. *J. Plant Biochem. Biotechnol.* **10**, 31–37.

Chen, C.J., Chen, H., Zhang, Y., Thomas, H.R., Frank, M.H., He, Y.H. and Xia, R. (2020) TBtools: an integrative toolkit developed for interactive analyses of big biological data. *Mol. Plant*, **13**, 1194–1202.

Chen, P.X., Zhi, F., Li, X.W., Shen, W.Y., Yan, M.J., He, J.Q., Bao, C.N. *et al*. (2022) Zinc-finger protein MdBBX7/MdCOL9, a target of MdMIEL1 E3 ligase, confers drought tolerance in apple. *Plant Physiol.* **188**, 540–559.

Collin, A., Daszkowska-Golec, A., Kurowska, M. and Szarejko, I. (2020) BarleyABI5 (abscisic acid insensitive 5) is involved in abscisic acid-dependent drought response. *Front. Plant Sci.* **11**, 1138.

Cutler, S.R., Rodriguez, P.L., Finkelstein, R.R., Abrams, S.R., Merchant, S., Briggs, W.R. and Ort, D. (2010) Abscisic acid: emergence of a core signaling network. *Annu. Rev. Plant Biol.* **61**, 651–679.

Dai, H.Y., Li, W.R., Han, G.F., Yang, Y., Ma, Y., Li, H. and Zhang, Z.H. (2013) Development of a seedling clone with high regeneration capacity and susceptibility to *Agrobacterium* in apple. *Sci. Hortic.* **164**, 202–208.

Farmer, L.M., Book, A.J., Lee, K.H., Lin, Y.L., Fu, H.Y. and Vierstra, R.D. (2010) The RAD23 family provides an essential connection between the 26S proteasome and ubiquitylated proteins in *Arabidopsis*. *Plant Cell*, **22**, 124–142.

Farooq, M., Wahid, A., Kobayashi, N., Fujita, D. and Basra, S.M.A. (2009) Plant drought stress: effects, mechanisms and management. *Agron. Sustain. Dev.* **29**, 185–212.

Finley, D. (2009) Recognition and processing of ubiquitin-protein conjugates by the proteasome. *Annu. Rev. Biochem.* **78**, 477–513.

Fryer, M.J., Oxborough, K., Mullineaux, P.M. and Baker, N.R. (2002) Imaging of photo-oxidative stress responses in leaves. *J. Exp. Bot.* **53**, 1249–1254.

Funakoshi, M., Sasaki, T., Nishimoto, T. and Kobayashi, H. (2002) Budding yeast dsk2p is a polyubiquitin-binding protein that can interact with the proteasome. *Proc. Natl Acad. Sci. USA*, **99**, 745–750.

Furihata, T., Maruyama, K., Fujita, Y., Umezawa, T., Yoshida, R., Shinozaki, K. and Yamaguchi-Shinozaki, K. (2006) Abscisic acid-dependent multisite phosphorylation regulates the activity of a transcription activator AREB1. *Proc. Natl Acad. Sci. USA*, **103**, 1988–1993.

Gabriely, G., Kama, R., Gelin-Licht, R. and Gerst, J.E. (2008) Different domains of the UBL-UBA ubiquitin receptor, Ddi1/Vsm1, are involved in its multiple cellular roles. *Mol. Biol. Cell*, **19**, 3625–3637.

Geng, D.L., Chen, P.X., Shen, X.X., Zhang, Y., Li, X.W., Jiang, L.J., Xie, Y.P. *et al*. (2018) *MdMYB88* and *MdMYB124* enhance drought tolerance by modulating root vessels and cell walls in apple. *Plant Physiol.* **178**, 1296–1309.

Gujjar, R.S., Karkute, S.G., Rai, A., Singh, M. and Singh, B. (2018) Proline-rich proteins may regulate free cellular proline levels during drought stress in tomato. *Curr. Sci.* **114**, 915–920.

Gujjar, R.S., Pathak, A.D., Karkute, S.G. and Supaibulwatana, K. (2019) Multifunctional proline rich proteins and their role in regulating cellular proline content in plants under stress. *Biol. Plant*, **63**, 448–454.

Guzder, S.N., Sung, P., Prakash, L. and Prakash, S. (1998) Affinity of yeast nucleotide excision repair factor 2, consisting of the Rad4 and Rad23 proteins, for ultraviolet damaged DNA. *J. Biol. Chem.* **273**, 31541–33154.

Hara, T., Kamura, T., Kotoshiba, S., Takahashi, H., Fujiwara, K., Onoyam, A.I., Shirakawa, M. *et al*. (2005) Role of the UBL-UBA protein KPC2 in degradation of p27 at G (1) phase of the cell cycle. *Mol. Cell. Biol.* **25**, 9292–9303.

Henry, A., Gowda, V.R.P., Torres, R.O., McNally, K.L. and Serraj, R. (2011) Variation in root system architecture and drought response in rice (*Oryza sativa*): phenotyping of the *OryzaSNP* panel in rainfed lowland fields. *Field Crop Res.* **120**, 205–214.

Huang, G.Q., Gong, S.Y., Xu, W.L., Li, P., Zhang, D.J., Qin, L.X., Li, W. *et al*. (2011) *GhHyPRP4*, a cotton gene encoding putative hybrid proline-rich protein, is preferentially expressed in leaves and involved in plant response to cold stress. *Acta Bioch. Biophys. Sin.* **43**, 519–527.

Huang, D., Wang, Q., Jing, G.Q., Ma, M.N., Li, C. and Ma, F.W. (2021) Overexpression of *MdIAA24* improves apple drought resistance by positively regulating strigolactone biosynthesis and mycorrhization. *Tree Physiol.* **41**, 134–146.

Hughes, J., Hepworth, C., Dutton, C., Dunn, J.A., Hunt, L., Stephens, J., Waugh, R. *et al*. (2017) Reducing stomatal density in barley improves drought tolerance without impacting on yield. *Plant Physiol.* **174**, 776–787.

Hunt, L., Amsbury, S., Baillie, A., Movahedi, M., Mitchell, A., Afsharinafar, M., Swarup, K. *et al*. (2017) Formation of the stomatal outer cuticular ledge requires a guard cell wall proline-rich protein. *Plant Physiol.* **174**, 689–699.

Huo, L.Q., Guo, Z.J., Zhang, Z.J., Jia, X., Sun, Y.M., Sun, X., Wang, P. *et al*. (2020) The apple autophagy-related gene *MdATG9* confers tolerance to low nitrogen in transgenic apple callus. *Front. Plant Sci.* **11**, 423.

Husnjak, K., Elsasser, S., Zhang, N.X., Chen, X., Randles, L., Shi, Y., Hofmann, K. *et al*. (2008) Proteasome subunit Rpn13 is a novel ubiquitin receptor. *Nature* **453**, 481–488.

Iglesias, A., Quiroga, S. and Diz, A. (2011) Looking into the future of agriculture in a changing climate. *Eur. Rev. Agric. Econ.* **38**, 427–447.

Ishii, T., Funakoshi, M. and Kobayashi, H. (2006) Yeast Pth2 is a UBL domain-binding protein that participates in the ubiquitin-proteasome pathway. *EMBO J.* **25**, 5492–5503.

Ishii, T., Funakoshi, M., Kobayashi, H. and Sekiguchi, T. (2014) Yeast Irc22 is a novel Dsk2-interacting protein that is involved in salt tolerance. *Cell*, **3**, 180–198.

Jia, X., Jia, X.M., Li, T.T., Wang, Y., Sun, X., Huo, L.Q., Wang, P. *et al*. (2021a) *MdATG5a* induces drought tolerance by improving the antioxidant defenses and promoting starch degradation in apple. *Plant Sci.* **312**, 111052.

Jia, X., Mao, K., Wang, P., Wang, Y., Jia, X.M., Huo, L.Q., Sun, X. *et al*. (2021b) Overexpression of *MdATG8i* improves water use efficiency in transgenic apple by modulating photosynthesis, osmotic balance, and autophagic activity under moderate water deficit. *Hortic Res.* **8**, 81.

Joo, J., Lee, Y.H. and Song, S.I. (2019) OsbZIP42 is a positive regulator of ABA signaling and confers drought tolerance to rice. *Planta*, **249**, 1521–1533.

Kang, Y., Vossler, R.A., Diaz-Martinez, L.A., Winter, N.S., Clarke, D.J. and Walters, K.J. (2006) UBL/UBA ubiquitin receptor proteins bind a common tetraubiquitin chain. *J. Mol. Biol.* **356**, 1027–1035.

Kim, J.H., Kim, M.S., Kim, D.Y., Amoah, J.N. and Seo, Y.W. (2022) Molecular characterization of U-box E3 ubiquitin ligases (TaPUB2 and TaPUB3) involved in the positive regulation of drought stress response in Arabidopsis. *Int. J. Mol. Sci.* **22**, 24.

Kishor, P.B.K., Kumari, P.H., Sunita, M.S.L. and Sreenivasulu, N. (2015) Role of proline in cell wall synthesis and plant development and its implications in plant ontogeny. *Front. Plant Sci.* **6**, 544.

Kito, K., Yeh, E.T.H. and Kamitani, T. (2001) NUB1, a NEDD8-interacting protein, is induced by interferon and down-regulates the NEDD8 expression. *J. Biol. Chem.* **276**, 20603–20609.

Lahari, T., Lazaro, J. and Schroeder, D.F. (2018) RAD4 and RAD23/HMR contribute to *Arabidopsis* UV tolerance. *Genes*, **9**, 8.

Lambertson, D., Chen, L. and Madura, K. (1999) Pleiotropic defects caused by loss of the proteasome-interacting factors Rad23 and Rpn10 of *Saccharomyces cerevisiae*. *Genetics*, **153**, 69–79.

Li, Y.Y., Mao, K., Zhao, C., Zhao, X.Y., Zhang, H.L., Shu, H.R. and Hao, Y.J. (2012) MdCOP1 ubiquitin E3 ligases interact with MdMYB1 to regulate light-induced anthocyanin biosynthesis and red fruit coloration in apple. *Plant Physiol.* **160**, 1011–1022.

Li, X.S., Zhang, J.H., Zhao, X.Y. and Liu, X.M. (2013) Protective effects of Rad23 protein on ultraviolet damage to HeLa cells. *J. Cent. South Univ.* **20**, 2974–2980.

Li, J.H., Ouyang, B., Wang, T.T., Luo, Z.D., Yang, C.X., Li, H.X., Sima, W. *et al*. (2016) *HyPRP1* gene suppressed by multiple stresses plays a negative role in abiotic stress tolerance in tomato. *Front. Plant Sci.* **7**, 967.

Li, L., Li, B., Xie, C., Zhang, T., Borassi, C., Estevez, J.M., Li, X.S. *et al*. (2020a) *Arabidopsis* RAD23B regulates pollen development by mediating degradation of KRP1. *J. Exp. Bot.* **71**, 4010–4019.

Li, X.W., Chen, P.X., Xie, Y.P., Yan, Y., Wang, L.P., Dang, H., Zhang, J. *et al*. (2020b) Apple SERRATE negatively mediates drought resistance by regulating MdMYB88 and MdMYB124 and microRNA biogenesis. *Hortic. Res.* **7**, 98.

Liang, R.Y., Chen, L., Ko, B.T., Shen, Y.H., Li, Y.T., Chen, B.R., Lin, K.T. *et al*. (2014) Rad23 interaction with the proteasome is regulated by phosphorylation of its ubiquitin-like (UbL) domain. *J. Mol. Biol.* **426**, 4049–4060.

Lin, Z., Li, Y., Wang, Y., Liu, X., Ma, L., Zhang, Z., Mu, C. *et al*. (2021) Initiation and amplification of SnRK2 activation in abscisic acid signaling. *Nat. Commun.* **12**, 2456.

Liu, S.X., Yu, Y.Z., An, H.Z., Li, N., Lin, N.S., Wang, W.Y., Zhang, W.P. *et al*. (2003) Cloning and identification of a novel ubiquitin-like protein, BMSC-UbP, from human bone marrow stromal cells. *Immunol. Lett.* **86**, 169–175.

Liu, D.Q., Han, Q., Shah, T., Chen, C.Y., Wang, Q., Tang, B.F. and Ge, F. (2018) A hybrid proline-rich cell-wall protein gene *JsPRP1* from juglans sigillata dode confers both biotic and abiotic stresses in transgenic tobacco plants. *Trees-Struct. Funct.* **32**, 1199–1209.

Liu, Y., Yang, T.Y., Lin, Z.K., Gu, B.J., Xing, C.H., Zhao, L.Y., Dong, H.Z. *et al*. (2019) A WRKY transcription factor *PbrWRKY53* from *Pyrus betulaefolia* is involved in drought tolerance and AsA accumulation. *Plant Biotechnol. J.* **17**, 1770–1787.

Liu, X.M., Jin, Y.B., Tan, K.X., Zheng, J.Z., Gao, T.T., Zhang, Z.J., Zhao, Y.J. *et al*. (2021) *MdTyDc* overexpression improves alkalinity tolerance in *Malus domestica*. *Front. Plant Sci.* **12**, 625890.

Ma, Y., Szostkiewicz, I., Korte, A., Moes, D., Yang, Y., Christmann, A. and Grill, E. (2009) Regulators of PP2C phosphatase activity function as abscisic acid sensors. *Science*, **324**, 1064–1068.

MacLean, A.M., Orlovskis, Z., Kowitwanich, K., Zdziarska, A.M., Angenent, G.C., Immink, R.G.H. and Hogenhout, S.A. (2014) Phytoplasma effector SAP54 hijacks plant reproduction by degrading MADS-box proteins and promotes insect colonization in a RAD23-dependent manner. *PLoS Biol.* **12**, e1001835.

Mellacheruvu, S., Tamirisa, S., Vudem, D.R. and Khareedu, V.R. (2016) Pigeonpea hybrid-proline-rich protein (CcHyPRP) confers biotic and abiotic stress tolerance in transgenic rice. *Front. Plant Sci.* **6**, 1167.

Mihaljevic, I., Viljevac Vuletic, M., Simic, D., Tomas, V., Horvat, D., Josipovic, M., Zdunic, Z. *et al*. (2021) Comparative study of drought stress effects on traditional and modern apple cultivars. *Plants*, **10**, 561.

Ning, D.L., Lu, T.C., Liu, G.F., Yang, C.P. and Wang, B.C. (2013) Proteomic analysis points to a role for RAD23 in apical dominance in *Pinus sylvestris* var. *mongolica*. *Plant Mol. Biol. Rep.* **31**, 1283–1292.

Ogura, T., Goeschl, C., Filiault, D., Mirea, M., Slovak, R., Wolhrab, B., Satbhai, S.B. *et al*. (2019) Root system depth in Arabidopsis is shaped by EXOCYST70A3 via the dynamic modulation of auxin transport. *Cell*, **178**, 400–412.e16.

Oh, J., Levy, J.G., Kan, C.C., Ibanez-Carrasco, F. and Tamborindeguy, C. (2022) CLIBASIA 00460 disrupts hypersensitive response and interacts with citrus Rad23 proteins. *Int. J. Mol. Sci.* **23**, 7846.

Pan, W.B., Lin, B.Y., Yang, X.Y., Liu, L.J., Xia, R., Li, J.G., Wu, Y.R. *et al*. (2020) The UBC27-AIRP3 ubiquitination complex modulates ABA signaling by promoting the degradation of ABI1 in Arabidopsis. *Proc. Natl. Acad. Sci. USA*, **117**, 27694–27702.

Park, S.Y., Fung, P., Nishimura, N., Jensen, D.R., Fujii, H., Zhao, Y., Lumba, S. *et al*. (2009) Abscisic acid inhibits type 2C protein phosphatases via the PYR/PYL family of START proteins. *Science*, **324**, 1068–1071.

Perez-Arellano, I., Carmona-Alvarez, F., Martinez, A.I., Rodriguez-Diaz, J. and Cervera, J. (2010) Pyrroline-5-carboxylate synthase and proline biosynthesis: from osmotolerance to rare metabolic disease. *Protein Sci.* **19**, 372–382.

Pitzschke, A., Datta, S. and Persak, H. (2014a) Salt stress in *Arabidopsis*: lipid transfer protein AZI1 and its control by mitogen-activated protein kinase MPK3. *Mol. Plant*, **7**, 722–738.

Pitzschke, A., Datta, S. and Persak, H. (2014b) Mitogen-activated protein kinase-regulated AZI1-an attractive candidate for genetic engineering. *Plant Signal. Behav.* **9**, e27764.

Pitzschke, A., Xue, H., Persak, H., Datta, S. and Seifert, G.J. (2016) Post-translational modification and secretion of Azelaic Acid Induced 1 (AZI1), a hybrid proline-rich protein from *Arabidopsis*. *Int. J. Mol. Sci.* **17**, 85.

Priyanka, B., Sekhar, K., Reddy, V.D. and Rao, K.V. (2010) Expression of pigeonpea hybrid-proline-rich protein encoding gene (*CcHyPRP*) in yeast and Arabidopsis affords multiple abiotic stress tolerance. *Plant Biotechnol. J.* **8**, 76–87.

Raymond, M.J. and Smirnoff, N. (2002) Proline metabolism and transport in maize seedlings at low water potential. *Ann. Bot.* **89**, 813–823.

Saikia, B., Singh, S., Debbarma, J., Velmurugan, N., Dekaboruah, H., Arunkumar, K.P. and Chikkaputtaiah, C. (2020) Multigene CRISPR/Cas9 genome editing of hybrid proline rich proteins (HyPRPs) for sustainable multi-stress tolerance in crops: the review of a promising approach. *Physiol. Mol. Biol. Plants*, **26**, 857–869.

Sasaki, S., Yamagishi, N. and Yoshikawa, N. (2011) Efficient virus-induced gene silencing in apple, pear and Japanese pear using Apple latent spherical virus vectors. *Plant Methods* **7**, 15.

Schultz, T.F. and Quatrano, R.S. (1997) Characterization and expression of a rice RAD23 gene. *Plant Mol. Biol.* **34**, 557–562.

Seo, S.G., Jeon, S.B., Kim, J.S., Shin, J.M., Kim, J.B., Kang, S.W., Lee, G.P. *et al*. (2011) Characterization and expression pattern of *IbPRP1* and *IbPRP2* stress-related genes from sweetpotato. *Genes Genom.* **32**, 487–497.

Stein, H., Honig, A., Miller, G., Erster, O., Eilenberg, H., Csonka, L.N., Szabados, L. *et al*. (2011) Elevation of free proline and proline-rich protein levels by simultaneous manipulations of proline biosynthesis and degradation in plants. *Plant Sci.* **181**, 140–150.

Stines, A.P., Naylor, D.J., Hoj, P.B. and van Heeswijck, R. (1999) Proline accumulation in developing grapevine fruit occurs independently of changes in the levels of delta (1)-pyrroline-5-carboxylate synthetase mRNA or protein. *Plant Physiol.* **120**, 923–931.

Sturm, A. and Lienhard, S. (1998) Two isoforms of plant *RAD23* complement a UV-sensitive *rad23* mutant in yeast. *Plant J.* **13**, 815–821.

Sun, X., Wang, P., Jia, X., Huo, L.Q., Che, R.M. and Ma, F.W. (2018) Improvement of drought tolerance by overexpressing *MdATG18a* is mediated by modified antioxidant system and activated autophagy in transgenic apple. *Plant Biotechnol. J.* **16**, 545–557.

Tsuchiya, H., Ohtake, F., Arai, N., Kaiho, A., Yasuda, S., Tanaka, K. and Saeki, Y. (2017) In vivo ubiquitin linkage-type analysis reveals that the Cdc48-Rad23/Dsk2 axis contributes to K48-linked chain specificity of the proteasome. *Mol. Cell*, **66**, 488–502.e7.

Umezawa, T., Sugiyama, N., Mizoguchi, M., Hayashi, S., Myouga, F., Yamaguchi-Shinozaki, K., Ishihama, Y. *et al*. (2009) Type 2C protein phosphatases directly regulate abscisic acid-activated protein kinases in Arabidopsis. *Proc. Natl. Acad. Sci. USA*, **106**, 17588–17593.

Wang, N., Gong, X.Q. and Ma, F.W. (2017) Genome-wide identification of the radiation sensitivity protein-23 (RAD23) family members in apple (*Malus* × *domestica* Borkh.) and expression analysis of their stress responsiveness. *J. Integr. Agr.* **16**, 820–827.

Wang, J., Qin, H., Zhou, S.R., Wei, P.C., Zhang, H.W., Zhou, Y., Miao, Y.C. *et al*. (2020) The ubiquitin-binding protein OsDSK2a mediates seedling growth and salt responses by regulating gibberellin metabolism in rice. *Plant Cell*, **32**, 414–428.

Wang, Y.P., Chen, Q., Zheng, J.Z., Zhang, Z.J., Gao, T.T., Li, C. and Ma, F.W. (2021) Overexpression of the tyrosine decarboxylase gene *MdTyDC* in apple enhances long-term moderate drought tolerance and WUE. *Plant Sci.* **313**, 111064.

Yang, K., An, J.P., Li, C.Y., Shen, X.N., Liu, Y.J., Wang, D.R., Ji, X.L. *et al*. (2021) The apple C2H2-type zinc finger transcription factor MdZAT10 positively regulates JA-induced leaf senescence by interacting with MdBT2. *Hortic Res.* **8**, 159.

Zhang, D.N., Chen, T., Ziv, I., Rosenzweig, R., Matiuhin, Y., Bronner, V., Glickman, M.H. *et al*. (2009) Together, Rpn10 and Dsk2 can serve as a polyubiquitin chain-length sensor. *Mol. Cell*, **36**, 1018–1033.

Zhang, X.L., Gong, X.Q., Li, D.Y., Yue, H., Qin, Y., Liu, Z., Li, M.J. *et al*. (2021a) Genome-wide identification of *PRP* genes in apple genome and the role of *MdPRP6* in response to heat stress. *Int. J. Mol. Sci.* **22**, 5942.

Zhang, H., Xue, Y.F., Yang, X., Liu, J. and Liu, Q. (2021b) *Toxoplasma gondii* UBL-UBA shuttle proteins regulate several important cellular processes. *FASEB J.* **35**, e21898.

Zhang, H., Yang, X., Ying, Z., Liu, J. and Liu, Q. (2021c) *Toxoplasma gondii* UBL-UBA shuttle protein DSK2s are important for parasite intracellular replication. *Int. J. Mol. Sci.* **22**, 7943.

Zhang, X.L., Gong, X.Q., Cheng, S.Y., Yu, H.X., Li, D.Y., Su, X.J., Lei, Z.L. *et al*. (2022) Proline-rich protein *MdPRP6* alters low nitrogen stress tolerance by regulating lateral root formation and anthocyanin accumulation in transgenic apple (*Malus domestica*). *Environ. Exp. Bot.* **197**, 104841.

Zhang, X.L., Gong, X.Q., Yu, H.X., Su, X.J., Cheng, S.Y., Huang, J., Lei, Z.L. *et al*. (2023) The proline-rich protein MdPRP6 confers tolerance to salt stress in transgenic apple (*Malus domestica*). *Sci. Hortic.* **308**, 111581.

Zhao, S., Gao, H.B., Jia, X.M., Li, X.W., Mao, K. and Ma, F.W. (2020) The gamma-clade HD-Zip I transcription factor *MdHB-7* regulates salt tolerance in transgenic apple (*Malus domestica*). *Plant Soil*, **463**, 509–522.

Zhou, K., Hu, L.Y., Li, Y.T.S., Chen, X.F., Zhang, Z.J., Liu, B.B., Li, P.M. *et al*. (2019) *MdUGT88F1*-mediated phloridzin biosynthesis regulates apple development and valsa canker resistance. *Plant Physiol.* **180**, 2290–2305.

Zhu, J.K. (2016) Abiotic stress signaling and responses in plants. *Cell*, **167**, 313–324.

Zhu, L.C., Li, B.Y., Wu, L.M., Li, H.X., Wang, Z.Y., Wei, X.Y., Ma, B.Q. *et al*. (2022) *MdERDL6*-mediated glucose efflux to the cytosol promotes sugar accumulation in the vacuole through up-regulating TSTs in apple and tomato. *Proc. Natl Acad. Sci. USA*, **118**, e2022788118.

Supporting information

Additional supporting information may be found online in the Supporting Information section at the end of the article.

Figure S1 Phylogenetic analyses of UBL-UBA proteins.
Figure S2 Identification of *MdRAD23D1* transgenic apple plants.
Figure S3 The ROS accumulation in wild type and *MdRAD23D1*-Ri transgenic plants under drought conditions.
Figure S4 Localization analyses of MdRAD23D1 and MdPRP6 using tobacco leaves, *Arabidopsis* protoplasts, and onion epidermal cells.
Figure S5 Identification of *MdPRP6* transgenic apple calli.
Figure S6 Identification of *MdPRP6* transgenic apple plants.
Figure S7 The ROS accumulation in wild type and *MdPRP6*-Ri transgenic apple plants under drought conditions.
Figure S8 MdRAD23D1 affects the protein abundance of MdPRP6.
Figure S9 Identification of *MdRAD23D1* transgenic apple calli.
Figure S10 Identification of co-transgenic apple calli.
Figure S11 Effects of mannitol treatment on the growth of wild type and *MdRAD23D1* transgenic apple calli.
Figure S12 Effects of exogenous proline on the stress response of wild type and *MdRAD23D1*-cRi calli.
Figure S13 Effects of P5CS pathway on the proline accumulation and stress response of wild type and *MdPRP6*-Ri plants.
Figure S14 Identification of *MdP5CS*-VIGS apple plants.
Figure S15 Effects of exogenous NDGA on the stress response of wild type and *MdPRP6*-Ri plants.
Table S1 Application of primers and sequences.

